Non-Solvability as a Physical Principle: A_5 and the Algebraic Origin of Information Barriers

Masaru Numagaki[1*]

[1]Independent Researcher, Kumamoto, Japan.

Corresponding author(s). E-mail(s): m.numagaki@medcure.co.jp;

Abstract

We consider a restricted model class in which microscopic three-dimensional geometry admits a finite rotation holonomy group $\boldsymbol{H} \leq \mathbf{SO(3)}$, and ask whether $\boldsymbol{H}$ can be uniquely determined from physical postulates alone.

Three postulates—Finiteness (H1), Irreducibility (H2), and Perfectness (H3)—motivated respectively by Planck-scale discreteness, the absence of privileged directions, and the absence of universal abelian charges, select $\boldsymbol{A_5}$ (the icosahedral rotation group of order 60) as the unique admissible holonomy under Klein's classification. Five logically independent sufficient conditions converge on the same conclusion, and the entire derivation chain is formally verified in Lean 4 (`sorry = 0`, `axiom = 0`).

The central result is not a derivation of the Standard Model, but a specification of falsifiable structural constraints. The representation theory of $\boldsymbol{A_5}$ yields a threefold prohibition structure defined by three independent mechanisms: a tensor-product selection rule for the four-dimensional irreducible representation $\boldsymbol{\rho_4}$ (P1), a multiplicity-free exclusion principle (P2), and a Coxeter-exponent filter derived from the exceptional Lie algebra $\boldsymbol{E_8}$ via the McKay correspondence (P3)—that pre-specifies the forbidden φ-power exponents $\boldsymbol{\{9, 15, 16, 25\}}$ with explicit algebraic reasons.

As a proof of concept, the pure $\mathbf{SU(3)}$ Yang–Mills one-loop coefficient $\boldsymbol{\beta_0 = 11}$ is reconstructed from icosahedral cell data as the identity $\boldsymbol{V - 1 \equiv E/n + \chi/2}$, a Type I (renormalization-group-invariant, hereafter RG-invariant) quantity immune to the scale problem. The scale problem is addressed by classifying RG survival mechanisms into Type I–III, with main-text claims restricted to Type I.

Keywords: $\boldsymbol{A_5}$, finite holonomy, Klein classification, prohibition structure, McKay Correspondence, Information barriers

Contents

1 Introduction

1.1 Motivation and scope

This paper investigates a restricted model class in which microscopic geometry in three spatial dimensions admits a finite rotation holonomy $H \leq \mathrm{SO}(3)$, and asks: can H be uniquely determined by physical principles alone—without fitting to empirical data?

The central question is whether the following logical chain is valid:

$$\text{Principles} \longrightarrow \text{Classification} \longrightarrow \text{Uniqueness}. \tag{1}$$

The conclusion is conditional. As long as (H1)–(H3) are adopted, $H \cong A_5$ remains unique within the framework of the Klein classification (Main Theorem). On the other hand, we do not claim to derive the Standard Model (SM) directly. Instead, the representation theory of A_5 yields a *prohibition structure* (also called the *index system* or the *exponent system* in earlier drafts): a pre-specification of "what must not appear" as a falsifiable constraint, determining which φ-power exponents are permitted and which are forbidden. Throughout this paper, the term *prohibition structure* is used exclusively.

The SM has more than 19 free parameters and does not explain why they take the values they do. The position of this paper is not to deny the SM, but to interpret it as a low-energy effective description of physics generated by the algebraic rigidity of A_5, and to argue against the fundamental existence of free parameters.

Limitations. The A_5 holonomy in this paper is a constraint on the exterior space and does not directly determine the interior gauge symmetry. The exterior–interior connection, the construction of the action functional, and the emergence of the continuum limit are addressed in Open Problem G1′ (Sect. 7, Appendix F).

1.2 Contributions (three core claims)

The contributions of this paper are limited to the following three claims.

Claim 1: Conditional uniqueness (Layer P → M). We formulate three postulates—finiteness (H1), irreducibility (H2), and perfectness (H3)—under independent motivation and show that A_5 is the only admissible holonomy selected by Klein's classification of finite rotation groups (Theorem 3.3). Furthermore, we show that five logically independent sufficient conditions converge to the same conclusion (Corollaries 3.4–3.7), ensuring the robustness of the conclusion (resistance to arbitrariness). This entire chain of reasoning is formally verified in Lean 4.

Claim 2: Minimal physical bridge (Type I proof of concept). As a Type I quantity independent of the RG scale, we reconstruct the pure SU(3) Yang–Mills $\beta_0 = 11$ from the icosahedral data (Sect. 4). The identity $V - 1 \equiv E/n + \chi/2$ eliminates arbitrariness in the choice of formula.

Claim 3: Falsifiable prohibition structure (Layer E core). From A_5 representation theory—the ρ_4 selection rule, the multiplicity-free condition, and the E_8 filter via McKay—the φ-exponents appearing in dimensionless constants are sorted into allowed and prohibited ranges (Sect. 6). The gap $= 1/\varphi^3$ is a quantity derived representation-theoretically from the character table (Sect. 4.1) and has no free parameters outside of A_5. What is important is not the "enumeration of matches" but the falsification form: "reject if the observed exponent falls within the forbidden index $\{9, 15, 16, 25\}$."

Other aspects—the exhaustive agreement of the constants table, the completion of the dynamical emergence to the SM, and detailed calculations of the frozen hypothesis along the history of the universe—are clearly separated as open problems (Sect. 7). Matters beyond the scope of this paper (such as the derivation of the SM, the dynamical mechanism, and the numerical proximity beyond chance in Appendix A) are explicitly listed in Sect. 7.1.

1.3 Epistemic contract: Layer M / P / E

To avoid confusion, the arguments in this paper are divided into three layers, and all subsequent discussions are governed by this contract.

Table 1 Three layers of epistemological separation.

Layer	Content	Verification method	Subject to refutation
Layer M (Mathematical theorems)	Theorem 3.1, Corollaries 3.1–3.2, Theorem 3.3, Corollaries 3.4–3.7, representation-theoretic calculations	Lean 4 + Mathlib (`sorry` = 0, `axiom` = 0)	Cannot be disproved (guaranteed by the type checker)
Layer P (Physical assumptions)	(H1) finite holonomy, (H2) irreducibility, (H3) perfectness	Theoretical consistency and indirect empirical evaluation	"Does nature belong to this model class?"
Layer E (Empirical correspondence)	Physical realization of prohibition structure, correspondence between allowed exponents and experimental values	Future precision measurements and new experiments	"Is the algebra of A_5 reflected in physical constants?"

This separation ensures that criticism of each layer does not spread to other layers. Even if the numerical proximity of Layer E turns out to be accidental, the theorems of Layer M and the conditional propositions of Layer P are not affected. Conversely, even if the assumptions of Layer P are empirically rejected, the mathematical content of Layer M continues to hold independently.

The position of formal verification. The mathematical reasoning in this paper—from the three principles to the uniqueness of A_5 and the entire process leading to the representation-theoretic consequences—has been machine-verified using Lean 4 [1] + Mathlib [2] (`sorry` = 0, `axiom` = 0). This allows criticism to focus on (a) the correctness of the Lean 4 type checker itself, or (b) the physical validity of the three principles. The theorem–Lean identifier correspondence table is included in the GitHub repository.

1.4 Falsifiability at a glance: what would refute this paper

The claims in this paper are separated into three layers (Layer M/P/E) with different modes of refutation.

(i) Layer M (irrefutable)

The theorems in Sect. 3 and the algebraic facts in Sect. 6 (character tables, tensor product decomposition, and prohibition structures) do not depend on empirical facts. What can be disproved is the Layer P/E hypothesis that "the mathematics is reflected in nature."

(ii) Layer P (falsification of the postulates)

(H1)–(H3) can be rejected independently. (H1) is refuted by evidence that the microscopic holonomy is a continuous group, (H2) by the existence of a universal fixed axis, and (H3) by the existence of a universal discrete charge. Detailed conditions for the refutation of each postulate are given in Sects. 2.2–2.4.

(iii) Layer E (most important: prohibition structure)

The core of our empirical argument is not an enumeration of coincidences but a *prohibition structure*. A selection rule derived from A_5 representation theory cuts off the allowable range of φ-power exponents, prohibiting a specific set of exponents: $\{9, 15, 16, 25\}$. If future precision measurements reveal that stable dimensionless ratios have φ^p relations corresponding to these prohibited exponents, the prohibition structure is immediately rejected.

Specific scenarios. (a) The system would be refuted if the absolute value of the neutrino mass ratio is determined (e.g. by DUNE) and the exponent p of m_{ν_3}/m_{ν_2} falls within the forbidden set. (b) It would also be refuted if the discovery of fourth-generation charged leptons is inconsistent with the constraints derived from McKay–E_8. (c) If the Higgs self-coupling constant λ_H is precisely measured after LHC Run 3 and the deviation from the ICO value is established at 5σ, its application to the electroweak sector would be rejected.

These scenarios are hypothetical, but the prohibition structure specifies clear rejection criteria in advance. In this respect, it is qualitatively different from fitting numbers after the fact.

(iv) Layer E (subsidiary)

The individual ICO values in Appendix A will be individually tested by future precision measurements, but the A_5 uniqueness in Sect. 3 and the prohibition structure (the algebra itself) in Sect. 6 will not be affected.

(v) Logical structure of refutation

- Layer M collapse ← Lean 4 type checker bug (effectively eliminated).
- Layer P collapse ← (H1) ∨ (H2) ∨ (H3) is rejected → the premise of the conditional theorem is lost.
- Layer E collapse ← violation of the prohibited index or significant deviation from numerical proximity → Layer M / Layer P are not affected.

1.5 Paper organization

The structure of this paper is as follows.

In Sect. 2, we formulate the model class and three postulates (H1)–(H3), and clarify the physical motivation and falsification conditions for each postulate. In Sect. 3, we prove the main theorem (the uniqueness of A_5) and verify its robustness using five independent convergence conditions. In Sect. 4, we present the icosahedral reconstruction for $\beta_0 = 11$ as a proof of concept, establishing the privileged status of Type I invariants. In Sect. 5, we directly address the scaling problem (G2) and clarify the scope of our claims through a Type I/II/III classification. In Sect. 6, we present the prohibition structure and derive the allowed/forbidden exponents using three layers: the ρ_4 selection rule, the multiplicity filter, and the E_8 Coxeter-exponent filter. In Sect. 7, we discuss limitations, compare with previous research, and organize open problems G1′–G6 into a prioritized research agenda. In Sect. 8, we draw conclusions. Appendix A contains protocolized observation logs (including A.12 Audit Summary) conforming to rules (R1)–(R3).

2 Model Class and Postulates

In this section, we define the model class under consideration and formulate three postulates (H1)–(H3), each of which is independently motivated and immediately followed by a falsification condition.

2.1 Defining the model class

This paper does not claim conclusions derived from general quantum gravity. We first state the limitation explicitly: the model class is restricted to those in which the micro-holonomy of the external space is expressed by a finite rotation group.

Discrete rotational symmetries in three-dimensional space have been completely classified by Klein [3]; see also Burnside [4] for the classical theory of finite groups. The finite subgroups of SO(3) fall into five families: the cyclic group C_n, the dihedral group D_n, the tetrahedral group A_4 (order 12), the octahedral group S_4 (order 24), and the icosahedral group A_5 (order 60).

The question in this paper is: *Can one of these five candidates be uniquely selected using only physically independent principles?*

The unifying motivation of the three principles: information finiteness. The three principles are not independent and arbitrary assumptions. They are positioned as stepwise constraints naturally motivated by the information-theoretic requirement that "microscopic geometry at the Planck scale can only hold a finite amount of information." The finiteness of information motivates the reduction from continuous groups to finite groups (H1), the isotropic maximal utilization of finite degrees of freedom requires the absence of privileged directions (H2), and the fact that the information barrier collapses to zero in solvable groups (Theorem 3.1) makes non-solvability inevitable (H3).

Each stage adds independent physical content—(H2) assumes an isotropic information distribution in space, and (H3) assumes the existence of irreversibility—but they are all motivated by the common requirement of finite information, which is consistent with the Bekenstein upper bound [5], the holographic principle, and several quantum gravity programs (Regge calculus [6], CDT [7], spin foam [8, 9]).

2.2 Postulate (H1): Finite holonomy (model class definition)

Statement. Microscopic local geometry has a finite subgroup $H \leq \mathrm{SO}(3)$ as its holonomy group:

$$H \leq \mathrm{SO}(3), \qquad |H| < \infty. \tag{2}$$

Physical motivation. (H1) is a model class-defining assumption, motivated by the natural emergence of discrete holonomies in discrete quantum gravity approaches (Regge calculus [6], CDT [7], spin foam [8, 9]), the finite information property due to the Bekenstein upper bound [5], and the nontrivial physical content of finite group lattice gauge theory [10].

Operational definition. In the three-dimensional Regge lattice, we assign an element $g_e \in H$ to the deficit angle of the triangle enclosing edge e in SO(3), and specify the geometric situation in which the range of the holonomy $h_\gamma = \prod_{e\in\gamma} g_e$ along a closed curve γ is restricted to a finite group.

What (H1) precludes. Continuous rotation groups only. Klein's classification limits the number of candidates to five.

Dimensional dependence. The choice of $n = 3$ is nontrivial. For $n = 2$ (SO(2)), the only finite subgroups are the cyclic groups C_m, and there are no non-solvable finite rotation groups, so the elimination method using (H2)(H3) itself fails. For $n = 4$ (SO(4)), the finite subgroups become enriched, making it difficult to achieve uniqueness via (H3). The gap $= 1/\varphi^4 \approx 0.146$ leads to $\alpha_s = \mathrm{gap}/2 = 0.073$ (a 38% deviation from the experimental value of 0.1180). $n = 3$ is a necessary condition for the gap $= 1/\varphi^3$ to be consistent with $\alpha_s(M_Z)$ within 0.03%.

Refutation condition. Conclusive evidence that the microscopic holonomy is a continuous group—direct observation of quantum gravitational effects without discrete rotational symmetry—would eliminate (H1). Indirectly, evidence for $n \neq 3$ also weakens (H1) (see quantitative collapse above).

Clarification of scope. This paper restricts itself to the holonomy of space frame bundles, excluding the spacetime holonomy (Lorentz/Spin(3, 1)). The lifting to Spin(3) $\cong$ SU(2) is treated as the binary icosahedral group $2I$ in Sect. 6.

2.3 Postulate (H2): Irreducibility (absence of locally privileged directions)

Statement. The natural action of H on $\mathbb{R}^3$ is irreducible:

$$\mathbb{R}^3 \text{ is irreducible as an } H\text{-module.} \tag{3}$$

Physical motivation. (H2) encodes the absence of locally privileged directions. When H acts reducibly, the invariant subspace defines a "special axis that is fixed in all microscopic rotations." (H2) eliminates the inherent anisotropy at this microscopic level, and is a stronger requirement independent of the statistical isotropy of random orientations (macro-isotropy).

Table 2 (H2) eliminates C_n and D_n; the polyhedral groups $\{A_4, S_4, A_5\}$ survive.

Group	3D representation	Invariant subspace	(H2)
C_n $(n \geq 2)$	Reducible	Rotation axis (1-dim.)	✗
D_n	Reducible	Main axis (1-dim.)	✗
A_4, S_4, A_5	Irreducible	None	✓

Refutation condition. If a universal fixed axis can be definitively confirmed at the single-cell level, then (H2) is rejected. If (H2) is violated, the five-fold symmetry disappears, φ disappears from the character table, and the entire prohibition structure of Sect. 6 collapses.

2.4 Postulate (H3): Perfectness (absence of universal abelian charges)

Statement. The abelianization of the holonomy group H is trivial:

$$H^{\mathrm{ab}} = H/[H, H] = 1. \tag{4}$$

Physical motivation. (H3) is the principle that "there is no universally definable abelian charge from microscopic holonomy." The sign homomorphism of S_4 automatically imparts a $\mathbb{Z}_2$ charge, and the quotient map $A_4 \to C_3$ of A_4 automatically imparts a $\mathbb{Z}_3$ charge. (H3) excludes this kind of automatically existing abelian conserved quantity.

Connections with symmetry constraints in quantum gravity. (H3) is structurally parallel to the No-Global-Symmetries Conjecture (Banks–Dixon [11]; Harlow–Ooguri [12]) and the Cobordism Conjecture (McNamara–Vafa [13]). The discrete charges automatically defined from $H^{\mathrm{ab}} \neq 1$ are nothing but discrete counterparts of the global symmetries eliminated in quantum gravity. However, both conjectures remain unproven, and strict equivalence with (H3) has not been established. This paper treats (H3) as an independent physical principle.

Structural alignment with Swampland conditions. The A_5 holonomy automatically satisfies the key conditions of the Swampland program—No-Global-Symmetries, Cobordism, Distance, and Finiteness—in a structural way. $H^{\mathrm{ab}} = 1$ forbids discrete global symmetries, and the absence of a continuous moduli space for discrete holonomies renders the assumption of the Distance Conjecture inapplicable. A systematic comparison is given in Appendix C.5.

Table 3 (H3) eliminates A_4 and S_4; only A_5 survives.

Group	H^{ab}	Automatic charge	(H3)
A_4	C_3	$\mathbb{Z}_3$ charge	✗
S_4	C_2	$\mathbb{Z}_2$ sign	✗
A_5	1	None	✓

Refutation condition. At the microscopic level, if the existence of a universal discrete charge ($\mathbb{Z}_2$ sign or $\mathbb{Z}_3$ phase) is confirmed, (H3) is disproved. If (H3) is violated and A_4 is adopted, $\alpha^{-1} \approx 27.4$ (80% deviation), $\Omega_{\mathrm{DM}}/\Omega_b = 3$ (43% deviation).

(H3) enhancement: solvable opacity (H3*). As we show in Sect. 3.1, (H3) is only the weakest shadow of the solvable probe analysis. A stronger property, (H3*), holds: any homomorphism from A_5 to a solvable group is trivial. On the candidate set $\{A_4, S_4, A_5\}$, (H3) and (H3*) are equivalent, but (H3*) has a wider scope as a physical principle.

Consistency with effective U(1)**.** (H3) does not deny low-energy U(1) symmetry; it only forbids the group-homomorphic image $H \to \mathrm{U}(1)$. An effective U(1) appears in the thermodynamic limit with many degrees of freedom.

2.5 Independence and acyclicity of the three principles

The three motivations are independent: (H1) is based on the definition of a model class, (H2) on local isotropy, and (H3) on the absence of universal charge. The exclusions are also non-overlapping—(H2) excludes C_n, D_n, and (H3) excludes A_4, S_4—so the three conditions function without redundancy. A_5 itself is not directly assumed. The fact that there are only five finite subgroups of SO(3) due to the Klein classification makes the uniqueness possible, but this does not occur for any pair of conditions alone (as will be refined in Sect. 3.5).

3 Main Theorem: Uniqueness of A_5 Holonomy in SO(3)

In this section, we prove that the three principles of Sect. 2 uniquely select A_5 in the Klein classification framework. In the first half, we briefly demonstrate the solvable opacity behind (H3), and in the second half, we establish the robustness of the main theorem via alternative conditions.

3.1 Solvable opacity

(H3) is the weakest shadow of a solvable probe analysis. To clarify this structure, the more general results are presented first.

Definition 3.1 (Solvable probe)**.** For a finite group G, a *solvable probe* is a group homomorphism $\pi\colon G \to Q$ to a solvable group Q. Physically, a solvable probe corresponds to an information channel defined by a finite-depth sequential measurement procedure—a hierarchical composition in which commuting outputs are used as inputs to select the observations of the next stage.

Theorem 3.1 (Opacity of solvable images)**.** Let G be a finite non-solvable group. Any solvable probe $\pi\colon G \to Q$ is non-injective.

Proof If π is injective, then $G \cong \pi(G) \leq Q$, and by subgroup inheritance of solvability, G is also solvable—a contradiction. *[Lean 4 verified.]* □

Corollary 3.1 (Complete degeneracy)**.** Let G be a finite simple group that is non-solvable. Any solvable probe $\pi\colon G \to Q$ is trivial: $\ker(\pi) = G$. For $G = A_5$, $|\ker(\pi)| = 60$. *[Lean 4 verified.]*

Corollary 3.2 (Cumulative opacity)**.** The product map of a finite family of solvable probes $(\pi_i\colon A_5 \to Q_i)_{i=1}^{k}$ is a constant map. No combination of finitely many solvable probes can distinguish any two elements in A_5. *[Lean 4 verified.]*

Theorem 3.2 (A_5 as a critical point)**.** All finite groups of order less than 60 are solvable, and A_5 (order 60) is the smallest non-solvable finite group. *[Lean 4 verified.]*

Corollary 3.3 (A_5 is the minimal basis for the information barrier)**.** (i) $|G| < 60 \Rightarrow G$ is solvable.
(ii) A_5 is non-solvable and exhibits complete invisibility with $|\ker| = 60$.
(iii) The A_5 barrier grows exponentially to $60^N \geq 2^{5N}$ in N steps.
[Lean 4 verified.]

Definition 3.2 (Solvable opacity (H3*))**.** (H3*) Solvable opacity. For a microscopic holonomy group H, any solvable probe $\pi\colon H \to Q$ is non-injective.

(H3*) is a strict strengthening of (H3) (since abelian groups $\subset$ solvable groups, (H3*) $\Rightarrow$ (H3)). In the candidate set $\{A_4, S_4, A_5\}$, they are equivalent—A_4, S_4 are solvable groups, so the identity map is an injective solvable probe and is eliminated.

Where is the novelty? Theorem 3.1 is the contrapositive of "a subgroup of a solvable group is solvable" and is a direct consequence of standard group theory. The contributions of this section are: (N1) reformulation as a physical principle (H3*), (N2) systematization of invisibility by combining Corollaries 3.1–3.2 and 3.3, and (N3) formal verification of the entire proof chain. The connection to computational complexity (Barrington, Krohn–Rhodes) is described in Appendix B.

3.2 Main theorem

Theorem 3.3 (A_5 holonomy uniqueness)**.** Under (H1) $\wedge$ (H2) $\wedge$ (H3), $H \cong A_5$.

Proof Assume $H \ncong A_5$. By Klein's classification theorem [3], $H \cong C_n$, D_n, A_4, or S_4. C_n and D_n are reducible, contradicting (H2). $A_4^{\mathrm{ab}} \cong C_3 \neq 1$ and $S_4^{\mathrm{ab}} \cong C_2 \neq 1$, contradicting (H3). In every case, a contradiction arises. *[Lean 4 verified.]* □

3.3 Robustness: alternative conditions

The same conclusion can be reached by replacing (H3) with any of four logically independent conditions. All of the following arguments assume that the candidates have been narrowed to $\{A_4, S_4, A_5\}$ by (H2).

Corollary 3.4 (Solvable opacity version)**.** (H1) $\wedge$ (H2) $\wedge$ (H3$*$) $\Rightarrow$ $H \cong A_5$. Since A_4, S_4 are solvable, the identity map is an injective solvable probe and eliminates them. *[Lean 4 verified.]*

Corollary 3.5 (Maximality version)**.** (H3′): Select the candidate with the highest order. A_5 is selected because $|A_4| = 12 < |S_4| = 24 < |A_5| = 60$.

Corollary 3.6 (Non-solvability version)**.** (H3″): H is non-solvable. A_4 and S_4 are solvable, so they are eliminated; only the non-solvable A_5 survives. *[Lean 4 verified.]*

Corollary 3.7 (Five-fold symmetry version)**.** (H3‴): H contains an element of order 5. The element orders of A_4 are $\{1, 2, 3\}$ and those of S_4 are $\{1, 2, 3, 4\}$, so they are excluded. A_5 contains an element of order 5 (e.g., (1 2 3 4 5)). *[Lean 4 verified.]*

Table 4 Comparison of five conditions. Each eliminates A_4 and S_4 by an independent mathematical mechanism, ensuring that A_5 selection is insensitive to axiom choice.

Condition	Formal pattern	Physical motivation	Exclusion mechanism
(H3) Perfectness	$H^{\mathrm{ab}} = 1$	Absence of universal abelian charges	Abelianization test
(H3*) Solvable opacity	Solvable probes are non-faithful	Fundamental limits of sequential measurement	Solvability test
(H3′) Maximality	$\lvert H\rvert$ maximal	Maximal utilization of microscopic structure	Order comparison
(H3″) Non-solvability	H is non-solvable	Existence of irreversibility	Solvability test
(H3‴) Five-fold symmetry	$\exists\, g \in H,\ \mathrm{ord}(g) = 5$	Existence of five-fold rotational symmetry	Element-order enumeration

3.4 Visualizing the elimination

The elimination cascade is summarized in Fig. 1.

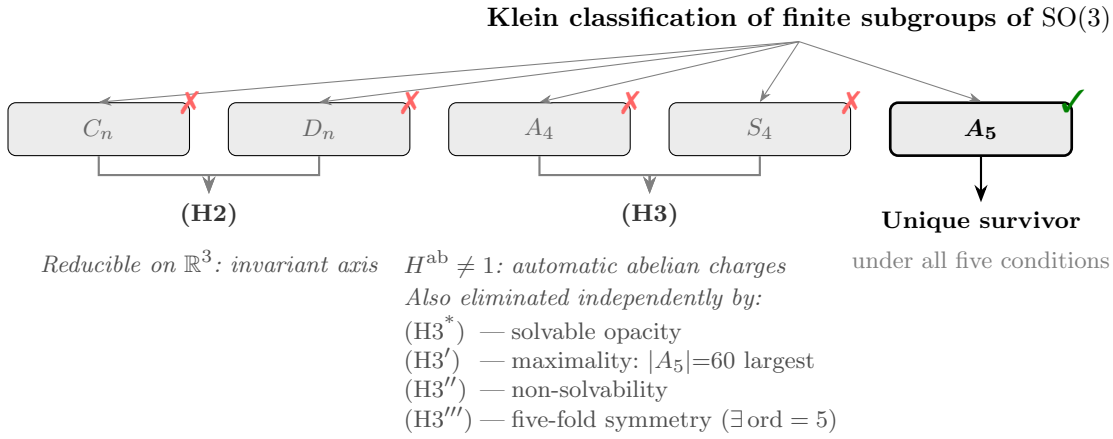

Fig. 1 Elimination cascade from Klein's classification to A_5. Postulate (H2) eliminates the cyclic and dihedral groups (reducible action), and postulate (H3) eliminates A_4 and S_4 (nontrivial abelianization). Five logically independent conditions all converge on A_5 as the unique surviving candidate

3.5 Strengths and limitations of the theorem

Strength. The elimination consists of the finite candidate property from the Klein classification, reducible-group exclusion via (H2), and the abelianization test of (H3); it is completely constructive. Corollaries 3.4–3.7 ensure that five different conditions converge to the same conclusion, and that the conclusion is insensitive to the choice of axioms (resistance to arbitrariness).

The mathematical nature of the theorem. The fact that A_5 is the only finite subgroup of SO(3) that is both irreducible and perfect is a consequence of the Klein classification and standard group theory. The

contribution of this paper is to reconstruct this fact as a stepwise elimination based on three independent physical principles. This provides a framework for evaluating the physical validity of each assumption individually.

Limitation. The physical necessity of (H1), (H2), and (H3) cannot be proven. These are axioms that define a model class of microscopic geometry, and their adoption is left to theoretical consistency and future empirical investigation.

On the smallness of the candidate space. The five constraints of the Klein classification make uniqueness possible—but not self-evident. Non-triviality resides in: (i) the exclusion targets of (H2)/(H3) being completely non-overlapping, (ii) the convergence of five independent algebraic characterizations (Sect. 3.3), and (iii) the physical motivation being independent of the conclusion.

Table 5 No pair of conditions alone suffices within the full physical framework; all three are needed.

Condition set	Surviving groups	Uniqueness?
(H1) ∧ (H2)	A_4, S_4, A_5	No (3 candidates)
(H1) ∧ (H3)	C_n, D_n, A_5	No (many candidates)
(H2) ∧ (H3)	A_5	Yes (but no reason to restrict to finite groups)

3.6 Status of formal verification

All theorems, corollaries, solvability tests, simplicity proofs, and order calculations in this section have been formally verified using Lean 4 (`sorry` = 0, `axiom` = 0). The only unformalized element is Klein's classification of finite rotation groups [3], which is cited as a classical theorem. The correspondence table is available in the GitHub repository.

4 Proof-of-Concept Bridge: Reconstructing $\beta_0 = 11$ from Icosahedral Data

$H \cong A_5$ is determined by Theorem 3.3. In this section, we first organize the discrete data derived from A_5 in Sect. 4.1, and then reconstruct the one-loop coefficient $\beta_0 = 11$ of the pure SU(3) Yang–Mills from the icosahedral data in Sects. 4.2–4.6, and show that this agreement is not an arbitrary choice of formula but is structurally necessary.

4.1 Algebraic data of A_5: icosahedral constants, φ, and representation theory

4.1.1 Orbit–stabilizer decomposition

From the transitive action of $A_5 \cong$ Rot(Icosahedron) on geometric elements and $|A_5| = |\text{Orbit}| \times |\text{Stab}|$:

Table 6 Orbit–stabilizer decomposition of A_5 acting on the icosahedron.

Geometric element	Stabilizer	Orbit equation	Value
Face F	$\mathbb{Z}_3$	$60/3 = 20$	20
Edge E	$\mathbb{Z}_2$	$60/2 = 30$	30
Vertex V	$\mathbb{Z}_5$	$60/5 = 12$	12

Euler's polyhedron formula $F + V - E = 2$ holds. The triple lock value $E/n = F/2 = |A_5|/6 = 10$ demonstrates the inherent overdetermination of the icosahedron. *[Verified.]*

Discrete Noether Correspondence (DNC). The orbit–stabilizer decomposition uniquely assigns three distinct stabilizer groups ($\mathbb{Z}_3$, $\mathbb{Z}_2$, $\mathbb{Z}_5$) to three geometric objects. Each stabilizer group defines topologically conserved discrete quantum numbers for the closed-curve holonomy and provides an algebraic basis for the correspondences to the force sectors: faces ($\mathbb{Z}_3$)→electromagnetic, edges ($\mathbb{Z}_2$)→strong

force, and vertices ($\mathbb{Z}_5$)→gravitational. However, ab initio derivation of this correspondence rule (C1) has not yet been achieved (L3, G3), and the choice of (C1) among the $3! = 6$ possible assignments is a posteriori. The perfectness (H3) ($H^{\mathrm{ab}} = 1$) prohibits automatic discrete conserved quantities at the A_5 level, while allowing the emergence of effective U(1) conservation laws in the continuous limit with many degrees of freedom—this two-layer structure of conservation laws is the physical core of DNC. The complete formulation of DNC is given in the Appendix.

4.1.2 Representation-theoretic derivation of φ, Galois deviation rate, and gap

Step 1: The occurrence of φ. A_5 has five conjugacy classes and the irreducible representation dimensions $\{1, 3, 3, 4, 5\}$ are determined. The character value $\chi_{\rho_3}(C_5)$ on the C_5 conjugacy class of ρ_3 is determined as a root of the minimal polynomial $x^2 - x - 1 = 0$ by the Schur orthogonality relation:

$$\chi_{\rho_3}(C_5) = \varphi = \frac{1+\sqrt{5}}{2}\,, \qquad \chi_{\rho_3}(C_5^2) = -\frac{1}{\varphi} = \frac{1-\sqrt{5}}{2}\,. \tag{5}$$

φ is uniquely determined solely from the group structure of A_5 and does not depend on any continuous parameters. *[Verified.]*

Step 2: Uniqueness of the Galois deviation rate λ_φ. φ and $-1/\varphi$ correspond to the Galois pair $\mathbb{Q}(\sqrt{5})/\mathbb{Q}$. Define the Galois deviation rate

$$\lambda_\varphi := |1 - \varphi| = \varphi - 1 = \frac{1}{\varphi} \approx 0.618\,. \tag{6}$$

As the following exhaustive check shows, λ_φ is the only non-trivial coupling parameter that the character table of A_5 allows—the only character value satisfying $0 < |\chi| < 1$.

Table 7 Exhaustive scan of character values. Only $1/\varphi$ on $\rho_3|_{C_5^2}$ satisfies $0 < |\chi| < 1$.

Repr.	Conj. class	χ	$\lvert\chi\rvert$	$0 < \lvert\chi\rvert < 1$?
ρ_3	C_5	$\varphi \approx 1.618$	> 1	No
ρ_3	C_5^2	$-1/\varphi \approx 0.618$	0.618	**Yes**
ρ_3	C_3	0	0	No (trivial)
ρ_3	C_2	-1	1	No (boundary)
ρ_4	C_5, C_5^2	-1	1	No
ρ_4	C_3	1	1	No
ρ_4	C_2	0	0	No
ρ_5	C_5, C_5^2	0	0	No
ρ_5	C_3	-1	1	No
ρ_5	C_2	1	1	No

Of all the nontrivial entries in the character table, only the value $1/\varphi$ on the conjugacy class of ρ_3, ρ_3' in the C_5 system satisfies $0 < |\chi| < 1$. *[Verified: `lambda_phi_unique_subunitary`.]*

Note that the definition of λ_φ, $|1-\varphi| = 1/\varphi$, is equivalent to the uniqueness condition of the character table, $|\chi_{\rho_3}(C_5^2)| = |-1/\varphi| = 1/\varphi$. In other words, λ_φ can be equivalently defined as "the absolute value of the ρ_3 character value on the C_5^2 conjugacy class," and this notation more directly shows the connection with the Galois structure below.

Remark 4.1 (Group-theoretic realization of the Galois action and structural consequences for λ_φ)**.** The Galois automorphism $\sigma\colon \sqrt{5} \mapsto -\sqrt{5}$ (i.e., $\varphi \mapsto -1/\varphi$) exchanging C_5 and C_5^2 is realized by the squaring map $g \mapsto g^2$, not by inversion $g \mapsto g^{-1}$. Specifically, traversing all 24 elements of order 5 in A_5:
(i) **Inversion preserves conjugacy classes:** $g \in C_5 \Longrightarrow g^{-1} \in C_5$ (similarly on the C_5^2 side).
(ii) **Squaring exchanges conjugacy classes:** $g \in C_5 \Longrightarrow g^2 \in C_5^2$ (the reverse also holds).
This is a direct reflection of the fact that $g^2 = g^{2 \bmod 5}$ corresponds to a Frobenius-type automorphism of $\mathrm{Gal}(\mathbb{Q}(\zeta_5)/\mathbb{Q})$. The map $g \mapsto g^{-1}$ has $g^{-1} = g^4 = g^{(-1) \bmod 5}$, and $-1 \equiv 4 \pmod 5$ belongs to the

subgroup $\{1, 4\}$ in $(\mathbb{Z}/5\mathbb{Z})^\times$, thus preserving the conjugacy class. On the other hand, 2 mod 5 corresponds to a nontrivial coset and realizes a Galois exchange. *[Verified:* `galois_action_realization` — `sorry` $= 0$, `axiom` $= 0$.*]*

Representation-theoretic foundation. Since ρ_3 is an orthogonal representation (real type), $\chi_{\rho_3}(g^{-1}) = \overline{\chi_{\rho_3}(g)} = \chi_{\rho_3}(g)$ holds for any $g \in A_5$. Hence inversion $g \mapsto g^{-1}$ leaves the character values unchanged and does not exchange φ and $-1/\varphi$.

On the other hand, the squaring map in (ii) sends $C_5 \to C_5^2$, so at the character level:

$$\chi_{\rho_3}(g) = \varphi \xrightarrow{g \mapsto g^2} \chi_{\rho_3}(g^2) = -\frac{1}{\varphi}\,, \tag{7}$$

which is exactly the representation-theoretic shadow of the Galois automorphism σ.

Structural consequences for λ_φ. This distinction defines the physical meaning of $\lambda_\varphi = 1/\varphi$. The operation connecting C_5 and C_5^2 is not an inversion (corresponding to a geometric reversal) but a squaring (corresponding to a Frobenius-type Galois action). Therefore, λ_φ is positioned as a "representation-theoretic trace of a Galois exchange on $\mathbb{Q}(\sqrt{5})/\mathbb{Q}$" rather than a "trace of a geometric inversion."

This structural distinction has two consequences. First, because the exchange $\varphi \leftrightarrow -1/\varphi$ cannot be achieved by a geometric operation (loop reversal), physical quantities governed by λ_φ (e.g., gap $= \lambda_\varphi^3$, hence α_s) are rooted in algebraic structures independent of spatial parity. Second, the physical distinction carried by C_5^+ and C_5^- has a different algebraic origin from the geometric C/P transformation. *[Verified:* `lambda_phi_galois_connection`*.]*

Step 3: Determinant scaling of the gap. $\rho_3 \colon A_5 \to \mathrm{GL}_3(\mathbb{C})$ is a 3-dimensional irreducible representation, and $\dim(\rho_3) = n = 3$ (spatial dimension) is a direct consequence of the fact that the icosahedron is a 3-dimensional object. On the C_5 conjugacy class, the eigenvalues of ρ_3 are $\{e^{2\pi i/5}, e^{-2\pi i/5}, 1\}$, but the Galois deviation acts equally in all eigendirections (due to irreducibility). By determinant scaling,

$$\text{gap} = \lambda_\varphi^{\dim(\rho_3)} = \left(\frac{1}{\varphi}\right)^3 = \frac{1}{\varphi^3} = \sqrt{5} - 2 \approx 0.2361\,. \tag{8}$$

[Verified: `gap_representation_theoretic_derivation`*.]*

Internal consistency check. The non-triviality of this derivation is ensured by the algebraic identity

$$\varphi^2 + \frac{1}{\varphi^2} = 3 = \dim(\rho_3)\,. \tag{9}$$

The fact that the right-hand side coincides with $\dim(\rho_3)$ is specific to A_5. Since $\varphi^2 - \varphi - 1 = 0$, we have $\varphi^2 = \varphi + 1$ and $1/\varphi^2 = 2 - \varphi$, so $\varphi^2 + 1/\varphi^2 = (\varphi + 1) + (2 - \varphi) = 3$. This equality implies that the sum of squares of the Galois deviation ratios reproduces the representation dimension, and the exponent "3" in λ_φ^3 is reconfirmed independently of $\dim(\rho_3)$. *[Verified:* `three_coincidence`*.]*

Collapse of alternative indices (gap index is uniquified to $n = 3$). We show the consequences if we adopt λ_φ^k $(k \neq 3)$ as the gap.

Table 8 Only $k = 3 = \dim(\rho_3) = n$ is consistent.

Index k	gap $= \lambda_\varphi^k$	$\alpha_s = \text{gap}/2$	$\alpha_s(M_Z)_{\text{exp}}$	Deviation
1	0.618	0.309	0.1180	162%
2	0.382	0.191	0.1180	62%
3	0.236	0.1180	0.1180	0.03%
4	0.146	0.073	0.1180	38%
5	0.090	0.045	0.1180	62%

$n = 3$ is an observational fact about the spatial dimension of the universe, and is not chosen a posteriori from the value of α_s. $k = 4$ corresponds to the assumption of four-dimensional space (SO(4)), but $\alpha_s = 0.073$ deviates from the experimental value by 38%.

Summary of derivation chain. In this derivation, the free parameters are zero. λ_φ is unique due to the character table, and the exponent $n = 3$ is fixed by the spatial dimension. The only remaining element is the determinant scaling hypothesis—that the Galois deviation rate raised to the power $\dim(\rho_3)$ controls the physical coupling parameters—classified as open problem G5.

4.1.3 Character table and tensor product rules

A_5 has five conjugacy classes, and five irreducible representations ρ_1, ρ_3, ρ_3', ρ_4, ρ_5 are determined. The character table is the algebraic basis for the prohibition structure of Sect. 6.

Table 9 Character table for A_5. $\varphi = (1+\sqrt{5})/2$. The character values of ρ_3, ρ_3' on the C_5 conjugacy class give two roots of $x^2 - x - 1 = 0$ by orthogonality, and generate φ algebraically.

	1	C_5 (12)	C_5^2 (12)	C_3 (20)	C_2 (15)
ρ_1	1	1	1	1	1
ρ_3	3	φ	$-1/\varphi$	0	-1
ρ_3'	3	$-1/\varphi$	φ	0	-1
ρ_4	4	-1	-1	1	0
ρ_5	5	0	0	-1	1

ρ_4 (4-dimensional, $A_5 = \mathrm{Alt}(5)$ standard representation) is the only irreducible representation that does not originate from SO(3) and is the basis for the ρ_4 selection rule (P1) in Sect. 6. The tensor product $\rho_4 \otimes \rho_4 = \rho_1 \oplus \rho_3 \oplus \rho_3' \oplus \rho_4 \oplus \rho_5$ contains all five irreducible representations exactly once.

Input summary. From $n = 3$ (spatial dimension) and A_5 (Theorem 3.3), we have $(F, E, V) = (20, 30, 12)$, φ, gap, and representation-theoretic data, all completely determined without continuous parameters.

4.2 Why target $\beta_0 = 11$ (Type I / RG-invariant)

The one-loop coefficient $\beta_0 = 11$ of the pure SU(3) Yang–Mills is suitable for checking the correspondence with the discrete structure because it is (i) integer-valued, (ii) directly linked to the strength of asymptotic freedom, and (iii) a Type I quantity independent of the RG scale. Even though the UV–IR coupling mechanism (G2, Sect. 5) remains unsolved, this agreement itself is a proof of concept that is not affected by the scaling problem.

4.3 Icosahedral reconstruction and the identity $V - 1 \equiv E/n + \chi/2$

The one-loop coefficient of pure SU(N_c) Yang–Mills is $\beta_0 = (11/3) \times 3 = 11$ when $n_f = 0$ and $N_c = 3$.

Using the icosahedron data $(V, E, F) = (12, 30, 20)$, $n = 3$, and $\chi = 2$,

$$\beta_0^{\mathrm{ICO}} = \frac{E}{n} + \frac{\chi}{2} = \frac{30}{3} + 1 = 11\,. \tag{10}$$

[Verified: `Ico_beta0_val`*.]*

Core defense: identity reduction to $V - 1$. $E/n + \chi/2$ is not an accidental numerical coincidence but an identity rewriting of the cohomological invariant $V - 1$ of the icosahedral sphere.

In a spherical triangulation, $3F = 2E$ (each face has three sides, each side is shared by two faces). From this and the Euler relation $V - E + F = \chi$,

$$V - 1 = \frac{E}{n} + \frac{\chi}{2} \tag{11}$$

is derived as an identity. *[Verified:* `Ico_beta0_decomposition`*,* `Ico_beta0_as_V_minus_one`*.]*

Connection to lattice gauge theory. $V - 1$ corresponds to the dimension of independent gauge transformations in lattice gauge theory (the number of gauge transformations on the vertices minus the

global constant transformation). Therefore,

$$\beta_0^{\mathrm{ICO}} = \frac{E}{n} + \frac{\chi}{2} = V - 1 = 11 \tag{12}$$

reduces to an identity that "expands the independent gauge transformation dimension $V - 1$ into the edge density and Euler characteristic."

The fermion coefficient also matches exactly:

$$\frac{|A_5|}{E\,n} = \frac{60}{30 \times 3} = \frac{2}{3} = 2\,T(R)\,. \tag{13}$$

[Verified: `Ico_quark_coeff`*.]*

4.4 Mechanical decomposition: 10 + 1 structural correspondence

The decomposition $\beta_0 = (10/3)\,C_2 + (1/3)\,C_2 = 10 + 1$ (transverse gluon + ghost) in the background field method of QCD is matched by the ICO decomposition $E/n + \chi/2 = 10 + 1$, term by term.

Table 10 The $10 + 1$ decomposition is preserved on both the QCD and ICO sides, suggesting a structural correspondence beyond mere numerical agreement.

QCD background field	ICO decomposition	Value
Dynamical: $(10/3)\,C_2 = 10$ (transverse gluon)	$E/n = 30/3 = 10$ (edge density)	10
Topological: $(1/3)\,C_2 = 1$ (ghost)	$\chi/2 = 2/2 = 1$ (Euler term)	1
Total: 11	Total: 11	11

4.5 Collapse in alternative groups

When computing β_0^{ICO} using the data for the three candidate polyhedral groups satisfying (H2), only the regular icosahedron reproduces $\beta_0 = 11$.

Table 11 Only the icosahedron (A_5) reproduces $\beta_0 = 11$, consistent with Theorem 3.3.

Group	Polyhedron	(V, E, F)	n	$E/n + \chi/2 = 11$?
A_4	Tetrahedron	$(4, 6, 4)$	3	3 ✗
S_4	Octahedron	$(6, 12, 8)$	3	5 ✗
A_5	Icosahedron	$(12, 30, 20)$	3	11 ✓

[Verified.]

4.6 Feedback to postulates (acyclicity)

The reconstruction of β_0 reinforces a posteriori that the settings of (H1)–(H3) are not arbitrary.

The point here is not a principle–conclusion cycle, but rather that the discrete data fixed in the main theorem fits with known Type I quantities as an independent consistency check.

5 The Scale Problem (G2): RG Survival Mechanisms and Main-Text Scope

In Sect. 4, $\beta_0 = 11$ is a Type I (RG-independent) quantity, bypassing the scaling problem. However, many of the exponent relations we will treat from Sect. 6 onward include quantities that are subject to RG running, such as coupling constants and mass ratios. In this section, we directly address the scaling problem (G2) and clarify the scope of the argument.

Table 12 Acyclicity check: the postulates are not derived from the result, but the result independently confirms their appropriateness.

Principle	A posteriori support from Sect. 4	If violated
(H1) Discreteness	Counting basis for $V - 1 = 11$	Cell counting impossible
(H2) Irreducibility	ρ_3 irreducible $\to$ SU(3) embedding scaffold	$N_c = n$ bridge collapses
(H3) Perfectness	Non-commutativity $\to$ consistency with asymptotic freedom ($\beta_0 > 0$)	$\beta_0 \neq 11$ (see Table 11)

5.1 Where the problem lies

The ICO values in this paper do not align to a single renormalization scale. α^{-1} is the Thomson limit, and α_s and $\sin^2\theta_W$ show best agreement near M_Z, with a scale difference of about five orders of magnitude. This paper decomposes G2 into three types.

5.2 Three types and test hypotheses

We classify the ICO-value preservation mechanisms into Types I–III and fix the test hypotheses and observational predictions for each.

Table 13 Classification of ICO quantities by RG survival mechanism and corresponding test hypotheses.

Type	RG preservation mechanism	Hypothesis	Observational prediction
I	Topological invariants (scale independence)	G2-A	$d\ln\alpha/(H_0\,dt)$ is constant at the ppb level
II	Universal quantities at fixed points	G2-C	Universal corrections near fixed points determine deviations from φ^p
III	Cosmological freeze-out	G2-B	The α_s/α ratio changes at high redshift, identifying the freeze-out epoch

The logic of this classification is straightforward. As long as at least one of the three types survives, there is room for the algebraic data of the discrete holonomy to be reflected at low energy. If all three types are rejected simultaneously, this corresponds to a negative solution of G2—a breakdown in the physical interpretation of the ICO system.

5.3 Conservative approach

(i) **The strong arguments in this paper are limited to Type I.** Type I consists of discrete integer data that is scale-independent by definition, and effectively bypasses G2.
(ii) **Type II/III are explicitly downgraded to test hypotheses.** They are separated from the logical core of the main theorem and the prohibition structure.

5.4 Type I (RG-invariant): integer-constructed constants

These quantities are not subject to RG running and are essentially free from the scaling problem. In particular, $\beta_0 = 11$ has structural significance as the icosahedral decomposition $E/n + \chi/2 = V - 1$, as shown in Sect. 4.3.

Table 14 Type I quantities: not subject to RG running and essentially free from the scaling problem.

ICO quantity	Value	Evidence for Type I
β_0 (n_f=0)	11 (exact)	One-loop coefficient is an integer.
		$E/n + \chi/2$ is topological.
Quark coefficient	2/3 (exact)	$\lvert A_5\rvert/(En)$ is a group-theoretic constant.
m_t/m_b	$E + V = 42$	Integer value, close to the pole mass ratio.

5.5 Type II (universal quantities at fixed points)

Type II is a hypothesis that universal quantities at RG fixed points are characterized by φ^p. Candidates are dimensionless pole mass ratios and cosmological ratios, and the deviations are larger (by several percent) than Type I.

Table 15 Type II candidates. Verifiable in principle by fixed-point analysis and lattice calculation.

ICO quantity	Value	Deviation	Basis
m_μ/m_e	φ^{11}	3.8%	Pole mass ratio
m_τ/m_e	φ^{17}	2.7%	Pole mass ratio
$\Omega_{\mathrm{DM}}/\Omega_b$	$\lvert A_5\rvert/V = 5$	6%	Cosmological ratio

These are positioned as research topics, not as established results.

5.6 Type III (cosmological freeze-out)

The Type III interpretation is that coupling constants are fixed in stages through different freeze-out processes for each physical quantity.

Table 16 Type III candidates. The scale inconsistency is a trace of differences in the freeze-out epoch, verifiable through high-redshift spectra and atomic clocks.

ICO quantity	Best-match scale	Deviation	Freeze-out candidate
$\alpha^{-1} = F\varphi^4$	Thomson limit	0.034%	IR limit of QED
$\alpha_s = \mathrm{gap}/2$	M_Z	0.03%	Electroweak scale
$\sin^2\theta_W$	M_Z ($\overline{\mathrm{MS}}$)	0.4%	EW symmetry breaking

5.7 Falsification protocol (G2)

Type I rejection. A quantity treated as Type I is rejected if it is established to be not scale-scheme independent.

Type II rejection. Rejection occurs when the φ^p constraint cannot be reproduced on the theoretical side (fixed-point analysis / lattice calculation) or is ruled out on the observational side.

Type III rejection. Rejection occurs when the predicted redshift dependence of α_s/α is observationally excluded.

The simultaneous rejection of all three types corresponds to a negative solution of G2—a breakdown in the physical interpretation of the ICO system.

6 The Prohibition Structure as Falsification Target

The core scientific argument of this section. The following numerical proximities are *not* the assertion of this section. The argument is for *prohibitions*—pre-specification of "what must not appear."

The representation theory of A_5 defines the allowed/forbidden boundaries of the φ-power exponents by three independent mechanisms (P1)–(P3). If a stable φ^p relation corresponding to the forbidden exponents $\{9, 15, 16, 25\}$ is established in the future, the system is immediately rejected.

6.1 Triple prohibition mechanism

The algebraic data for A_5 established in Sect. 4.1 (character table, tensor product rules, and exterior algebra) lead to the following three independent prohibition mechanisms.

(P1) ρ_4 selection rule. Of the 10 nontrivial tensor products, only three non-self-products containing ρ_4 on one side give dimensions corresponding to exponents of physical constants. The remaining seven (dimensions $\{9, 15, 16, 25\}$) are prohibited.

(P2) Multiplicity-free condition. Seven of the eight symmetric/alternating squares correspond to exponent sets with multiplicity 1. The only exception is $\mathrm{Sym}^2(\rho_5) = \rho_1 \oplus \rho_4 \oplus 2\rho_5$ (multiplicity > 1), which is prohibited. It functions as the A_5 version of the exclusion principle.

(P3) E_8 Coxeter-exponent filter. Of the eight Coxeter exponents of E_8, only $\{11, 17\}$ can be derived independently from the icosahedral parameters, while the remaining six cannot be directly excited in the three-dimensional A_5 projection.

The intersection of the threefold prohibition structures defines the index set S. The scientific value of the system lies in the predictive power of the prohibition structure—the ability to pre-specify what should not appear. Numerical proximity is documented in Appendix A, but is secondary to the falsifiability of the system.

Refutation condition. If the φ-exponents of newly discovered physical constants violate (P1)–(P3)—if a stable φ^p relation corresponding to the forbidden dimensions $\{9, 15, 16, 25\}$ is established—the system is rejected.

6.2 ρ_4 selection rule (P1)

There are 10 nontrivial tensor products $\rho_i \otimes \rho_j$ $(i, j \geq 2,\ i \leq j)$ of A_5, uniquely determined by the representation ring (there is no a posteriori choice).

Rule. The dimension of the product belongs to the exponent set S if and only if (C1) $\rho_4 \in \{\rho_i, \rho_j\}$ and (C2) $\rho_i \neq \rho_j$ (it is not a self-product).

Algebraic reasons for each prohibition. $\{9, 15, 25\}$ (ρ_4-free): These are products of representations derived from SO(3) and do not inject any information specific to the non-solvable structure of A_5. This is a representation-theoretic reflection of the solvable opacity of Sect. 3.1, where the information of A_5 disappears in a solvable probe.

$\{16\}$ ($\rho_4 \otimes \rho_4$, self-product): A "maximum entropy decomposition" that includes all five irreducible representations once, and does not have the ability to select specific physical quantities. It is the only tensor product whose decomposition contains ρ_1, by the Schur orthogonality relation.

Table 17 ρ_4 selection rule (P1). 10/10 perfect match. The only allowed tensor product dimensions are $\{12, 20\} = \{V, F\}$.

Tensor product	Dim.	Contains ρ_4?	Self-product?	$\in S$?	
$\rho_3 \otimes \rho_3$	9	N	Y	Forbidden	✓
$\rho_3 \otimes \rho_3'$	9	N	N	Forbidden	✓
$\rho_3 \otimes \rho_4$	12	Y	N	Allowed	✓
$\rho_3 \otimes \rho_5$	15	N	N	Forbidden	✓
$\rho_3' \otimes \rho_3'$	9	N	Y	Forbidden	✓
$\rho_3' \otimes \rho_4$	12	Y	N	Allowed	✓
$\rho_3' \otimes \rho_5$	15	N	N	Forbidden	✓
$\rho_4 \otimes \rho_4$	16	Y	Y	Forbidden	✓
$\rho_4 \otimes \rho_5$	20	Y	N	Allowed	✓
$\rho_5 \otimes \rho_5$	25	N	Y	Forbidden	✓

Specificity of ρ_4. ρ_4 is the only irreducible representation that does not originate from SO(3) (Sect. 4.1.3), and the rule that an intersection with ρ_4 is necessary to inject A_5-specific information into

the physical exponent can be interpreted as a representation-theoretic reflection of the solvable opacity of Sect. 3.1.

Systematic elimination of alternative rules. None of the six naturally assumed alternative rules (e.g., "products involving ρ_3," "even dimensions only," "non-self-products only," etc.) achieves 10/10. (C1) $\wedge$ (C2) is the only rule in the examined rule class that gives an exact match (see Appendix B for details).

Conservative probability assessment. If one randomly assigns 10 tensor products to 6 distinct dimension values, the probability of getting exactly 3 in $\{12, 20\}$ and 7 that do not is $p \approx 0.83\%$ (hypergeometric distribution).

6.3 Multiplicity-free condition (P2) and five-layer classification

(P2) Contents. Of the eight symmetric/alternating squares, seven correspond to exponent sets with multiplicity 1. The only exception is $\mathrm{Sym}^2(\rho_5)$ (containing $2\rho_5$), which is prohibited.

Five-layer classification. The exponent set S can be completely described as the union of the following five layers:

Table 18 Five-layer classification of the exponent set S. Layers A–D are rigorously derived from A_5 representation theory and the E_8 connection. Layer E consists of multiplicative and additive compositions of Layers A–D with gradually weakened structural constraints.

Layer	Mathematical mechanism	Indices	Physical sector
A	Irreducible representation dimension	$\{4\}$	Gauge coupling fundamental scaling
B	Symmetric/alternating power (multiplicity-free)	$\{3, 6, 10\}$	Force, mixing angle, mass ratio
C	ρ_4 cross tensor product	$\{12, 20\} = \{V, F\}$	QCD scale, neutrinos
D	E_8 exponent, icosahedral filter	$\{11, 17\}$	Charged lepton mass
E	Algebraic closure of icosahedral arithmetic	$\{8, 42, 48, 70, 204, \ldots\}$	Cosmology and gravity

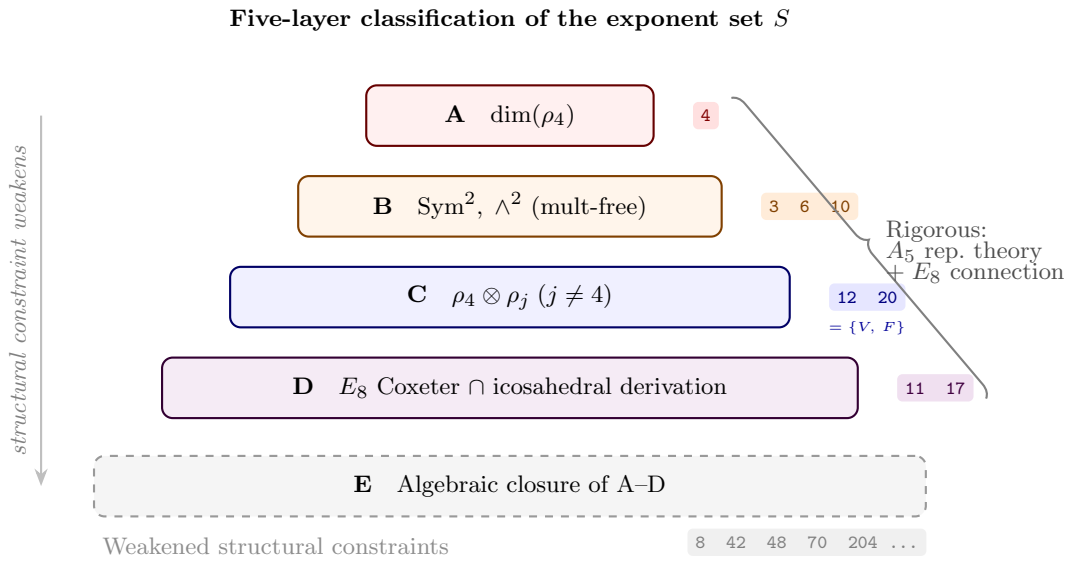

Fig. 2 Five-layer classification of the exponent set S. Width represents the strength of the structural constraint: Layer A (narrowest) is derived directly from the dimension of ρ_4, while Layer E (widest, dashed) consists of algebraic compositions with gradually weakened constraints. Layers A–D are rigorously derived from A_5 representation theory and the E_8 connection; Layer E extends through multiplicative and additive closure

6.4 E_8 connection and dual membership filter (P3)

Lifting to Spin(3) $\cong$ SU(2) gives the binary icosahedral group $2I$ of order 120, the double cover of A_5. By the McKay correspondence (1980) [14], $2I$ corresponds uniquely to the affine E_8 Dynkin diagram.

Layer D structure. Of the Coxeter exponents $\{1, 7, 11, 13, 17, 19, 23, 29\}$ of E_8, only $\{11, 17\}$ can be independently derived as known physical combinations of icosahedral parameters.

Table 19 Dual membership: both E_8 Coxeter exponents and independent icosahedral combinations.

E_8 exponent	Icosahedral derivation	Physical quantity
11	$\beta_0 = E/n + \chi/2 = V - 1$	$m_\mu/m_e \approx \varphi^{11}$
17	$F - n = 20 - 3$	$m_\tau/m_e \approx \varphi^{17}$

This dual membership—being both an E_8 Coxeter exponent and an independent icosahedral combination—distinguishes $\{11, 17\}$ from all other E_8 exponents.

Numerical necessity of the McKay correspondence. The Coxeter number $h(E_8) = 30 = E$ is a direct consequence of the McKay correspondence and ensures that the appearance of E_8 is inseparable from the icosahedral structure ($\sum m_i = 30$, $\sum m_i^2 = 120 = |2I|$). A candidate path from E_8 to the SM ($E_8 \supset E_6 \supset \mathrm{SU}(3)^3$) is an open problem in G1′ (emergence problem). Details of the McKay correspondence, the representation theory of $2I$, and a comparison with Lisi are given in Appendix C.

6.5 Summary of prohibited indices and falsification protocol

Table 20 Prohibited indices and their exclusion mechanisms. Each prohibition traces to one or more of (P1)–(P3).

Prohibited index	Mechanism	Algebraic reason
9	(P1)	ρ_4-free: only solvable components from SO(3)
15	(P1)+(P2)	ρ_4 absent; $\mathrm{Sym}^2\rho_5$ has multiplicity > 1
16	(P1)	$\rho_4 \otimes \rho_4$ (self-product): includes all 5 irreducibles, hence no selectivity
25	(P1)	ρ_4 absent and self-product

Falsification protocol. The system is rejected if a dimensionless ratio R corresponding stably to a forbidden index $p \in \{9, 15, 16, 25\}$ establishes $|R/\varphi^p - 1| < 1\%$, or if the 10/10 agreement of the ρ_4 selection rule breaks down with the discovery of new structures.

6.6 Breakdown of prohibition structures in alternative groups

The prohibition structure (P1)–(P3) is unique to A_5 and does not hold for other Klein candidates. A_4 (four irreducible representations, dimensions $\{1, 1, 1, 3\}$) has only one tensor product and the selection rule degenerates, while S_4 (five irreducible representations, dimensions $\{1, 1, 2, 3, 3\}$) lacks a non-SO(3)-derived irreducible representation, and the premise of (P1) disappears. Neither group has φ in its character values. Only A_5 simultaneously satisfies (a) five irreducible representations, (b) a non-SO(3)-derived ρ_4, and (c) character value φ.

6.7 Representative numerical proximity (selection) and reference to Appendix A

While this section argues for a prohibition structure, it would be incomplete to entirely omit the correspondence with observations. Below, we present only representative examples, primarily Type I (RG-independent); a complete list of approximately 46 entries is included in the protocolized observation log in Appendix A.

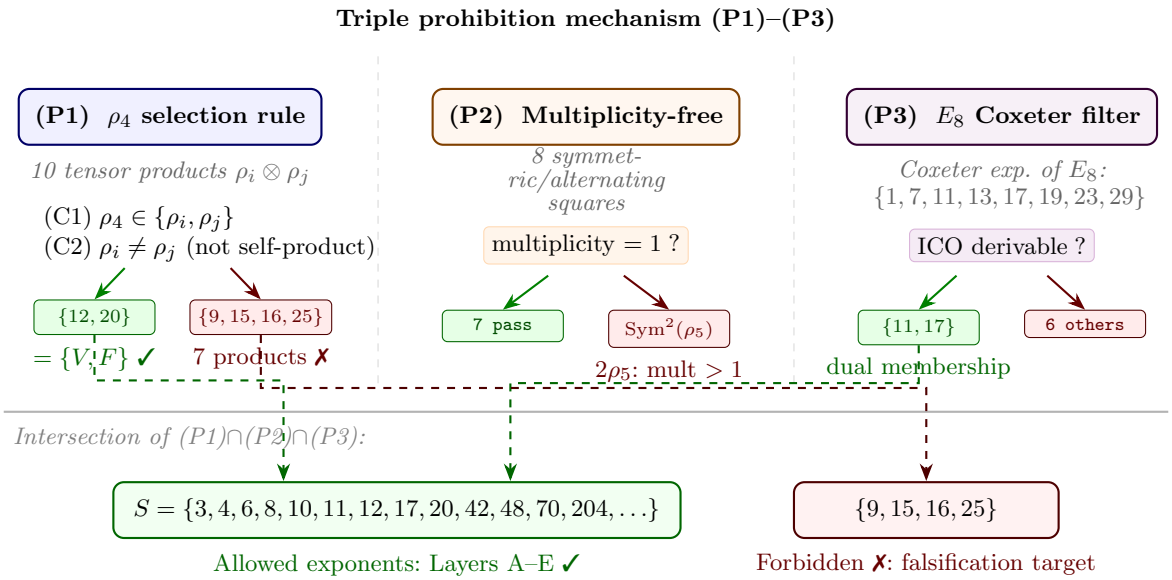

Fig. 3 Triple prohibition mechanism (P1)–(P3) and its role as a falsification target. The ρ_4 selection rule (P1) filters tensor products by requiring ρ_4 involvement in non-self-products; the multiplicity-free condition (P2) excludes $\mathrm{Sym}^2(\rho_5)$; the E_8 Coxeter filter (P3) retains only dual-membership exponents $\{11, 17\}$. The intersection defines the allowed exponent set S, while the forbidden indices $\{9, 15, 16, 25\}$ serve as pre-registered falsification targets

Table 21 Representative numerical proximity (selected). The Type column corresponds to the RG survival classification in Sect. 5.

#	Quantity	ICO formula	ICO value	Exp.	Dev.	Type
1	α^{-1}	$F\varphi^4$	137.08	137.036	0.034%	I/III
2	$\alpha_s(M_Z)$	gap/2	0.1180	0.1180(9)	0.03%	I/III
3	β_0 (n_f=0)	$E/n + \chi/2$	11	11	exact	I
4	m_μ/m_e	φ^{11}	199.0	206.8	3.8%	II
5	m_τ/m_e	φ^{17}	3571	3477	2.7%	II
6	m_t/m_b	$E + V = 42$	42	41.5	1.2%	I
7	$\Omega_{\mathrm{DM}}/\Omega_b$	$\lvert A_5\rvert/V$	5.0	5.3(1)	$\sim$6%	II

Notes. #1 and #2 share a closure relation, joining at $\alpha_s \cdot \alpha^{-1} = 10\varphi$ (the triple lock value). The exponents $\{11, 17\}$ of #4 and #5 are the E_8 dual assignments in Sect. 6.4. The systematic increase in deviation from Type I (exact to 0.03%) to Type II (2–6%) is consistent with the mechanism classification in Sect. 5.

Limitations. (a) The correspondence rule (C1) has not been derived from first principles (G3). (b) The ICO values are not aligned to a single scale (G2, Sect. 5). (c) $\sin^2\theta_W \approx \mathrm{gap} = 2\alpha_s$, so these are not independent. There is no correspondence to the CP phase.

6.8 Epistemological summary of this section and terms of use for Appendix A

The argument in Sect. 6 is limited to two points:

(i) The representation theory of A_5 provides a closed description system for φ-power exponents, and there are non-trivial selection rules and a hierarchy (an algebraic fact).

(ii) This system has a falsifiable prohibition structure (P1)–(P3) (pre-registered falsification conditions).

The dynamical mechanism (G4), the derivation of the correspondence rule (G3), and the scale problem (G2) are explicit non-assertions.

Appendix A operating terms. Appendix A complements the logical core of the main text (A_5 uniqueness, prohibition structures, and Type I proof of concept) as an audit log, not as the core of the evidence. To prevent reactive responses and double counting, all items are assigned a protocol (R1)–(R3): Role (Input I / Selection S / Prediction P / Derivation D / Exploration X / Tension T), Type (I/II/III), and Forb (prohibition index check). Items used for selection are not counted as successes, and prohibition

index violations are kept as negative controls (see A.12). Numerical proximity is not used in the inference of A_5 (the inference direction is reversed), and the falsifiable content of the system is encoded in the prohibition/permission structure.

7 Limitations, Prior Work, and Open Problems

In this section, we frankly list the limitations of this paper, briefly highlight differences from previous research, and present open problems G1′–G7 as a prioritized roadmap.

7.1 What this paper does not claim (explicit listing of limitations)

The following items are outside the scope of this paper and no claims are made.

(L1) Lack of dynamical mechanism. It is unclear how the algebraic structure of A_5 is translated into observables. This paper provides "algebraic constraints," not "dynamics."

(L2) Absence of external–internal gauge connection. A_5 holonomy is a constraint on the exterior space and does not directly determine the interior gauge symmetry $\mathrm{SU}(3) \times \mathrm{SU}(2) \times \mathrm{U}(1)$. The McKay path ($2I \to E_8 \to \mathrm{SU}(3)^3$) only indicates the existence of a candidate path, but is not a dynamical derivation (G1′).

(L3) Non-derivability of correspondence rules. The correspondence rule (C1) (faces → electromagnetic, edges → strong force, vertices → gravity) is not derived from first principles (G3). The choice of (C1) among the $3! = 6$ possible assignments is a posteriori, and the numerical table in Sect. 6.7 cannot escape this a posteriori status.

(L4) Scale issues. Although we decomposed the problem into three types (Type I–III) in Sect. 5, it is not yet clear which conservation mechanism is physically realized (G2). All correspondences other than Type I (integer structural constants) remain hypotheses to be tested.

(L5) Dynamical basis of determinant scaling. In the derivation of gap $= \lambda_\varphi^{\dim(\rho_3)} = 1/\varphi^3$ (Sect. 4.1.2), we established the uniqueness of λ_φ, $\dim(\rho_3) = 3$, and that λ_φ is a representation-theoretic signature of the Galois exchange ($C_5 \leftrightarrow C_5^2$ via $g \mapsto g^2$). What remains unresolved is the dynamical basis of determinant scaling (G5).

(L6) Absence of CP phase. A_5 has only real representations and does not naturally generate complex phases. The structure corresponding to CP violation is beyond the scope of this paper. Note that the reality of ρ_3 is also the representation-theoretic basis for $\chi_{\rho_3}(g^{-1}) = \chi_{\rho_3}(g)$ (inversion preserves conjugacy classes; see Remark 4.1 (i)), and is inseparably related to the Galois structure of L5.

(L7) Unformalized Klein classification. The only unformalized proposition in the argument chain. Once completed, the entire argument will be machine-verifiable from end to end.

7.2 Comparison with previous studies

The geometric derivation of coupling constants has a long history. We briefly highlight the methodological differences.

Wyler (1969). Derived $\alpha^{-1} \approx 137.036$ from the volume ratio of a symmetric space, but there is no mathematical necessity for the choice of symmetric space (Gilmore's criticism). In this paper, A_5 is uniquely determined by elimination from the three principles.

Atiyah (2018). Attempted a derivation of α^{-1} using the $6j$ symbol, but the work is incomplete. It shares the focus on A_5 representation theory, but differs in that the reasons for choosing A_5 are explicitly discussed here.

Koide (1981). The empirical formula for charged lepton masses gives $Q = 2/3$. In this paper, $m_\mu/m_e = \varphi^{11}$, $m_\tau/m_e = \varphi^{17}$, $Q \approx 0.6655$ (deviation 0.2%), and the formal equivalence to $Q = 2/3 = 1 - 1/n$ suggests a connection with spatial dimensions.

Lisi (2007). Starts from E_8 as a direct assumption. In this paper, E_8 is a consequence of the McKay correspondence and is not an assumption. Distler–Garibaldi's criticism [15] does not directly apply to the connection path in this paper (see Appendix C.6 for details).

Differences from discrete quantum gravity approaches. Regge calculus, CDT, and spin foam all start with discretization as an "approximation of a continuum theory," with physical constants input as parameters of the action. Our approach reverses this logic: we treat finite group holonomy as a fundamental entity, and the uniqueness established by the three principles (Theorem 3.3) completely eliminates the degrees of freedom of the discretization, allowing algebraic data to constrain the physical constants. However, our approach is positioned as a complement to discrete quantum gravity, not a replacement.

Novelty of this paper. The mathematical content itself is not new (the central result of Sect. 3 is a known contrapositive, and the algebra in Sect. 6 is a standard fact of A_5 representation theory). The novelty lies in the three-stage reconstruction: (N1) reformulation as a physical principle (H3*), (N2) systematization of robustness through multi-path convergence of the five conditions, and (N3) connection to the prohibition structure (P1)–(P3). In the context of *Foundations of Physics*, the core contribution is the question itself: "Why does a known theorem reappear as a physical principle?"

7.3 Open problems G1′–G7: prioritized roadmap

Research strategic priorities.

Top priorities: G2 (scale issues) and G6 (physical realization). G2 can be systematically tackled through the three-type analysis in Sect. 5, and influences the physical interpretation of the entire system. G6 is the only problem that can be experimentally explored independently of G1′.

Second priority: G3 (correspondence) and G4 (index). The internal consistency of the algebraic structure of A_5 can be explored independently of G1′.

Core issues: G1′ (emergence) and G5 (gap). The most fundamental but also the most difficult.

Table 22 Open problems G1′–G7: prioritized research roadmap.

Problem	Content	Priority	Strategy route
G1′	Emergence: dynamical derivation $A_5 \to$ SM	Core	McKay path $2I \to E_8 \to E_6 \to \mathrm{SU}(3)^3$ (L2 unsolved). String-theoretic candidates: $\mathbb{C}^2/2I$ ADE singularity (I), heterotic $E_8 \times E_8$ (II) (Appendix F, G7).
G2	Scale issue: identifying RG survival mechanisms	Highest	Sect. 5 Type I–III analysis, lattice calculations
G3	Correspondence: first-principles derivation of (C1)	2nd	Structural correspondence between stabilizer orders $\{3, 2, 5\}$ and gauge rank
G4	Index problem: dynamical basis of prohibition structures	2nd	First-principles derivation of ρ_4 selection rule (G4′)
G5	Determinant scaling: dynamical basis of $\lambda_\varphi^{\dim(\rho_3)}$	Core	Discrete holonomy $\leftrightarrow$ field theory connection (subproblem of G1′)
G6	Physical realization: experimental search for solvable opacity	Highest	A_5 gauge theory anyons, interference experiments
G7	String theory consistency: $2I \hookrightarrow E_8$ verification	2nd	ADE singularities, heterotic embeddings, Dechant construction (Appendix F)

Formulation of each problem.

G1′ (emergence problem). From the algebraic rigidity of A_5, construct a framework that directly describes the segmentation of forces, the hierarchy of matter, and the scale structure without free parameters. The gauge group of the SM is not a goal to be achieved, but should be recovered a posteriori as a low-energy effective description of the physics generated by A_5.

G2 (scale problem). See the three-type analysis in Sect. 5. Type I is solved, Type II is theoretically explorable, and Type III is observationally testable.

G3 (correspondence problem). First-principles derivation of the correspondence rule (C1). The structural correspondence between the stabilizer group orders $\{3, 2, 5\}$ and the gauge group rank, and the triple lock value $10 = E/n = F/2 = |A_5|/6$ are key clues.

G4 (index problem). The dynamical basis of the prohibition structure in Sect. 6. Why specific physical quantities are assigned specific φ-power exponents. The first-principles derivation of the ρ_4 selection rule is formulated as sub-problem G4′.

G5 (determinant scaling problem). Dynamical basis for $\lambda_\varphi^{\dim(\rho_3)} = 1/\varphi^3$ (see L5). It was established in Sect. 4.1.2 that λ_φ is a representation-theoretic trace of the Galois exchange $\sigma\colon \varphi \mapsto -1/\varphi$, realized group-theoretically by $g \mapsto g^2$. What remains unresolved is the dynamical basis for why λ_φ raised to the $\dim(\rho_3)$ power controls the physical coupling parameters. Candidate approaches: (i) spectral analysis of the ρ_3 determinant in the plaquette action of discrete gauge theories, (ii) saddle-point approximation of the partition function in the A_5 version of Dijkgraaf–Witten theory [16]. This is a subproblem of G1′.

G6 (physical realization of solvable opacity). The most direct problem connecting the no-go theorem of Sect. 3.1 to experimental exploration: (i) anyons in A_5 gauge theory (non-solvable phases in discrete gauge theories), and (ii) quantum computation tasks specific to A_5 (interference experiments on phase factors that do not appear in solvable groups).

G7 (string theory integration). Consistency checks of the $A_5 \to 2I \to E_8$ chain with the standard E_8 construction of superstring theory. (G7a) Calculation of the $2I \hookrightarrow E_8$ centralizer group. (G7b) Compactification interpretation of forbidden indices. (G7c) Connection between Dechant's $3 \to 8$ dimensionality increase and critical dimensions. Details are given in Appendix F.

Interrelationships of open problems. The development of G1′ naturally subsumes G3, but G3 and G4 can be explored independently of G1′ as problems on the algebraic internal structure of A_5. The solution of G2 directly affects the interpretation of G4 and G5. G6 can be explored independently of G1′ and is the problem closest to experiment, based on Sect. 3.1.

7.4 Information barriers and entropy (preview)

The solvable opacity in Sect. 3.1 shows that the 60 elements of A_5 cannot be distinguished by solvable probes, generating an exponential information barrier of $60^N \geq 2^{5N}$ in N steps. This suggests: (i) a group-theoretic reinterpretation of the Boltzmann entropy (an algebraic basis for coarse-graining), (ii) an algebraic basis for irreversibility (a solvable-group universe has zero information barrier), and (iii) a formal connection to the cosmological constant ($\Lambda\ell_{\mathrm{Pl}}^2 \sim \varphi^{-600}$, $600 = 2 \times 291 + (E - V)$). All of these are speculative interpretations (Layer P/E), and details are provided in Appendix D.

8 Conclusion

8.1 Summary of key findings

This paper proves that the holonomy group A_5 is uniquely selected under the three principles (H1)–(H3) (Theorem 3.3, robust due to the convergence of five conditions, Lean 4 formally verified), and obtains the following consequences.

(i) **Proof of concept (Sect. 4).** $\beta_0^{\mathrm{ICO}} = E/n + \chi/2 = V - 1 = 11$ (identity).

(ii) **Prohibition structure (Sect. 6).** Pre-registration of the forbidden exponents $\{9, 15, 16, 25\}$ by (P1)–(P3).

(iii) **Decomposition of the scaling problem (Sect. 5).** Type I–III classification. The main text focuses on Type I.

8.2 The structure of conditional consequences

The focus of this paper is not to assert that "A_5 is true," but to list the necessary conditions for a φ-power system to hold as three layers, and to provide independent falsification conditions for each layer.

Layer 1 (Existence conditions). φ does not appear if any of three-dimensionality, non-solvability, irreducibility, or the perfect group property is missing (Theorem 3.3).

Layer 2 (Structural conditions). The ρ_4 selection rule, the multiplicity-free condition, and the E_8 Coxeter-exponent filter form the prohibition structure.

Layer 3 (Consistency conditions). Micro and macro are connected by inter-sector consistency relations such as $\beta_0 = V - 1 = 11$.

Each layer can be independently falsified.

Five Cosmic Constraints. The above three layers are unified into five constraints: (CC1) information barrier, (CC2) symmetry segmentation, (CC3) prohibition structure, (CC4) necessity of scale hierarchy, and (CC5) cosmological consistency, based on the single algebraic fact that A_5 is the smallest non-solvable finite simple group (Appendix E).

8.3 What is established and what remains unresolved

Table 23 Established results (top) and unresolved problems (bottom).

Established result	Epistemic status
A_5 uniqueness (Theorem 3.3, Corollaries 3.4–3.7)	Layer M (formally verified)
Solvable opacity (Theorem 3.1, Corollaries 3.1–3.2)	Layer M (formally verified)
Algebraic facts of the prohibition structure (P1)–(P3)	Layer M (derived from character table and tensor products)
$\beta_0 = V - 1 \equiv E/n + \chi/2 = 11$	Layer M (identity, formally verified)
Unresolved problem	**Reference**
Dynamical mechanism ($A_5 \to$ observables)	G1′ (Sect. 7.3)
Scale issue (identifying RG survival mechanisms)	G2 (Sect. 5, Sect. 7.3)
Deriving the correspondence rules	G3 (Sect. 7.3)
Dynamical basis of the prohibition structure	G4 (Sect. 7.3)
Dynamical basis of determinant scaling	G5 (Sect. 7.3)
Experimental verification of solvable opacity	G6 (Sect. 7.3)

8.4 Outlook

The core questions boil down to two: why (H1)(H2)(H3) are physically plausible, and by what mechanism the discrete structure of A_5 is translated into observables. For the former, $\beta_0 = 11$ (Sect. 4.3) provides a posteriori support, and the prohibition structure (Sect. 6) provides falsifiability. For the latter, a research program is formulated as G1′–G7.

The mathematical chain $A_5 \to 2I \to E_8$ is structurally consistent with standard constructions of superstring theory (Appendix F). Why the algebraic rigidity of A_5—the smallest non-solvable finite simple group—resonates with so many physical structures is a question beyond the scope of this paper. This paper provides a rigorous starting point for exploring that question: a set of formally verified theorems, a pre-registered list of falsification conditions, and prioritized open problems.

Acknowledgments. The formal verification in this paper is based on the Lean 4 theorem prover [1] and the Mathlib mathematical library [2]. The author thanks the developer communities of both projects.

Statements and Declarations.

Funding.

This research received no external funding.

Competing interests.

The author declares no competing interests.

Ethics approval and consent to participate.

Not applicable.

Consent for publication.

Not applicable.

Data availability.

This paper contains no experimental data. All numerical values of physical constants referenced in this work are taken from published sources cited in the bibliography.

Materials availability.

Not applicable.

Code availability.

The complete Lean 4 source code for the formal verification (sorry = 0, axiom = 0) and the theorem–identifier correspondence table are publicly available at https://github.com/nuu/A5CosmicNecessity under the Apache License 2.0. The repository includes all files necessary to reproduce the verification: `lakefile.lean`, Mathlib dependency specifications, and per-section Lean source files (`Section1_Introduction.lean` through `Section8_Conclusion.lean` and auxiliary modules).

Author contribution.

M. Numagaki is the sole author and is responsible for the conception of the theoretical framework, all mathematical proofs and their Lean 4 formalization, the numerical analysis, and the writing of the manuscript.

Use of AI-assisted tools.

Use of Generative AI and AI-assisted technologies in the writing process During the preparation of this work the author used ChatGPT in order to improve the readability and language of the manuscript. After using this tool/service, the author reviewed and edited the content as needed and takes full responsibility for the content of the publication.

Appendix A Protocolized Observation Log

A complete list (46 items) of correspondences between ICO formulas and physical constants constructed from the discrete algebraic structure of A_5. This appendix follows the terms of use in Sect. 6.8 and complements the logical core of the main text (A_5 uniqueness, prohibition structure, Type I proof of concept). It is operated as an audit log.

A.1 Protocol definitions (R1)–(R3)

To prevent retroactive counting and double counting, all 46 items are assigned the following three protocol columns.

(R1) Role. Each item is classified into six categories to structurally prevent inflation of "success rates."
(R2) Type (RG survival category). Each item's preservation mechanism under RG flow is classified according to the three types of Sect. 5.
(R3) Forb (prohibition index check). Match against the forbidden set $\{9, 15, 16, 25\}$ of Sect. 6.5. Items falling within the forbidden index are isolated as T (negative control) and excluded from the allowed set S_{allowed}.

Input summary. From $n = 3$ (spatial dimension) and A_5 (Theorem 3.3): $(F, E, V) = (20, 30, 12)$, $\varphi = (1 + \sqrt{5})/2$, $|A_5| = 60$, $\chi = 2$, gap $= 1/\varphi^3$. The single dimensional input is $M_Z = 91.19$ GeV.

Table A.1 (R1) Role classification.

Role	Meaning	Constraint
I	Input (fixed)	Cannot be included in success rate or prediction count
S	Selection set (used to calibrate C1)	Cannot be included in success rate or prediction count
P	Predictive holdout	Candidates that the text can reference as "achievements"
D	Derived (depends on other items)	Cannot be counted as an independent prediction. Dependency noted in Dep column.
X	Exploratory (uncertain/undetermined)	Immature. Promote to P or reject in the future.
T	Tension / negative control	Retained as a failure example. Negative control for the prohibition structure.

Table A.2 (R2) RG survival type.

Type	Meaning	Main-text status
I	RG-independent (integer/topological)	Subject of main-text strong argument
II	Fixed point / universal quantity hypothesis	Downgraded to test hypothesis
III	Cosmic freeze-out / scale dependence	Downgraded to observation programme

Legend. Deviation = $|(\text{ICO} - \text{obs})/\text{obs}|$. φ-exp = φ exponent. Ly = five-layer classification (A–E) from Sect. 6.3. Forb: ✓ = allowed, △ = falls in forbidden set, — = no exponent. Dep: — = independent, ↗# = depends on item #.

A.2 Gauge coupling constants and scales

Table A.3 Gauge coupling constants and scales (#1–#10).

#	Quantity	ICO formula	ICO	Exp.	Dev.	φ-e	Ly	R	Ty	Dep
1	α^{-1}	$F\varphi^4$	137.08	137.036	0.034%	4	A	S	II	—
2	$\alpha_s(M_Z)$	gap/2	0.1180	0.1180	0.03%	3	B	S	II	—
3	$\sin^2\theta_W$	gap$(1-1/(F\pi))$	0.2312	0.2312	0.4%	3	B	P	II	—
4	α/α_G	φ^{204}	$\sim 10^{44}$	$\sim 10^{44}$	∼2%	204	E	P	II	—
5	α_s/α	10φ	16.18	16.16	<0.1%	—	—	D	II	↗1,2
6	$\beta_0(n_f{=}0)$	$E/n{+}\chi/2$	11	11	exact	—	—	P	I	—
7	Quark coeff.	$\lvert A_5\rvert/(En)$	2/3	2/3	exact	—	—	P	I	—
8	Λ_{QCD}	M_Z/φ^{12}	283 MeV	292 MeV	3.1%	12	C	P	III	—
9	M_{Pl}/m_e	$\sqrt{F}\,\varphi^{104}$	$\sim 2.4{\times}10^{22}$	$\sim 2.4{\times}10^{22}$	∼1.6%	104	E	D	III	↗4
10	M_{GUT}/M_Z	φ^{68}	$\sim 10^{14}$	$\sim 10^{14}$	order	68	E	D	III	↗4

Note. #1 and #2 are used to select the correspondence rule (C1), so Role = S. #5 is the ratio of #1 and #2 and is a derivative. #6 and #7 are RG-independent integers/rationals (Type I), and are the core of the proof of concept in Sect. 4.

A.3 Charged lepton masses

Note. #11 depends on #1 (α) and #27 (M_Z), hence D. The exponents $\{11, 17\}$ of #12 and #13 are the E_8 dual assignments (Layer D) of Sect. 6.4. #14 is a derived quantity depending on #12 and #13.

Table A.4 Charged lepton masses (#11–#14).

#	Quantity	ICO formula	ICO	Exp.	Dev.	φ-e	Ly	R	Ty	Dep
11	m_e	$M_Z\alpha^2(1-\alpha)/(n\pi)$	0.511 MeV	0.511 MeV	0.2%	—	—	D	II	↗1,27
12	m_μ/m_e	φ^{11}	199.0	206.8	3.7%	11	D	P	II	—
13	m_τ/m_e	φ^{17}	3571	3477	2.7%	17	D	P	II	—
14	Koide Q	$1-1/n = 2/3$	0.6667	0.6666	0.01%	—	—	D	II	↗12,13

Table A.5 Quark masses (#15–#20).

#	Quantity	ICO formula	ICO	Exp.	Dev.	φ-e	Ly	R	Ty	Dep
15	m_t	$M_Z\varphi^2/\sqrt{2}\cdots$	172.8 GeV	172.6 GeV	0.14%	2	—	P	II	—
16	m_t/m_b	$F+V+E/n = 42$	42	41.5	1–2%	42	E	P	II	—
17	m_t/m_c	φ^{10}	123.0	134(±)	scheme	10	B	P	II	—
18	m_c/m_s	$V+\varphi$	13.62	13.6(±)	∼0.2%	—	—	D	II	↗17
19	m_s/m_d	$F = 20$	20	20(±)	∼0.2%	20	C	D	II	↗18
20	m_d/m_u	$\sqrt{5}$	2.236	2.16(±)	∼3.5%	—	—	P	II	—

A.4 Quark masses

Note. Quark masses have large uncertainty due to scheme dependence. The ICO value of #16 is an integer (42), but the physical quantity m_t/m_b itself is a pole mass ratio with scheme dependence, so it is classified as Type II.

A.5 Neutrino masses (exploratory)

Table A.6 Neutrino masses (#21–#23).

#	Quantity	ICO formula	ICO	Exp.	Dev.	φ-e	Ly	R	Ty	Dep
21	m_{ν_3}	$(m_e^2/M_Z)\varphi^{-8}$	∼0.06 eV	∼0.05 eV	∼22%	8	E	X	III	—
22	m_{ν_2}/m_{ν_3}	φ^{-6}	0.056	∼0.17	×3	6	B	X	III	—
23	m_{ν_1}/m_{ν_2}	φ^{-11}	0.005	upper lim.	—	11	D	X	III	↗22

Note. Normal ordering assumed. Absolute mass is uncertain; Role = X due to large experimental uncertainty. Next-generation experiments such as DUNE can upgrade or reject these entries.

A.6 Mixing angles

Note. #26 is the only item for which φ-exp = 9 falls in the forbidden set $\{9, 15, 16, 25\}$. It is isolated as Role = T (negative control). The deviation of factor ∼3 is a positive signal of the soundness of the prohibition rule—the absence of precise agreement for physical quantities corresponding to forbidden exponents is consistent with the predictions of (P1)–(P3).

A.7 Electroweak boson masses

Note. #27 is the only dimensional input (Role = I). #30 is a derived quantity depending on #29 and #27.

A.8 Higgs sector

Note. #33 is X because the experimental value is not yet confirmed. It can be tested by precise measurement of the Higgs self-coupling constant after LHC Run 3 (Sect. 1.4 (iii)(c)).

Table A.7 Mixing angles (#24–#26).

#	Quantity	ICO formula	ICO	Exp.	Dev.	φ-e	Ly	R	Ty	Dep
24	$\sin\theta_C$	gap	0.2361	0.2253	4.8%	3	B	X	II	—
25	$\sin^2\theta_{13}(\nu)$	$2/(5\varphi^6)$	0.0223	0.0218	2.3%	6	B	X	II	—
26	$\lvert V_{ub}\rvert$ suppression	gap^3	0.013	0.004	$\times 3$	9	—	T	II	—

Table A.8 Electroweak boson masses (#27–#30).

#	Quantity	ICO formula	ICO	Exp.	Dev.	φ-e	Ly	R	Ty	Dep
27	M_Z	Reference scale	91.19 GeV	91.19 GeV	—	—	—	I	—	—
28	M_W/M_Z	$\sqrt{2/\varphi}$	0.874	0.882	0.9%	—	—	P	II	—
29	v (VEV)	$M_Z\varphi^2$	238.7 GeV	246.2 GeV	3%	2	—	P	II	—
30	$G_F^{-1}\sqrt{2}$	$M_Z^2\varphi^4$	$\sim 1.09\times10^5$	$\sim 1.17\times10^5$	6.3%	4	A	D	II	↗29

Table A.9 Higgs sector (#31–#33).

#	Quantity	ICO formula	ICO	Exp.	Dev.	φ-e	Ly	R	Ty	Dep
31	m_H/M_Z	$\varphi - \text{gap}$	1.382	1.374	0.6%	—	—	P	II	—
32	m_H/M_W	$\approx \varphi$	1.581	1.559	$\sim$0.2%	—	—	D	II	↗28,31
33	λ_H	$(\varphi-\text{gap})^2/(2\varphi^4)$	0.140	—	—	—	—	X	II	↗31

A.9 Hadron masses

Note. #34 depends on #8 (Λ_{QCD}). #35 is doubly dependent on #11 and #34, and has high accuracy (0.002%) but no independent predictive power.

A.10 Gravity and the Planck scale

Note. #36 and #37 depend on inputs #1 and #27 via #11 (m_e). #38 has digit-level precision, hence X.

A.11 Cosmological parameters

Note. The index 600 of #39 indicates inter-sector consistency as $2 \times 291 + (E-V) = 600$ (Sect. 7.4, CC5). #43 is a derived quantity dependent on #39 and #37.

A.12 Dark components and baryon asymmetry (speculative)

Note. All items in this section are X (Exploratory). The physics of dark matter and dark energy is still uncertain, and their correspondence with the ICO system is speculative.

A.13 Audit summary

The purpose of this appendix is not to display a "match success rate" but, under (R1)–(R3), to clarify what is input, what is selection, what is prediction, what is derivation, and to isolate items contradicting the prohibition index as T (negative control).

A.13.1 Role breakdown (#1–#46)

A.13.2 RG type breakdown

A.13.3 Prohibition index check (Forb)

The forbidden set is $\{9, 15, 16, 25\}$ (Sect. 6.5). In this log, only index 9 appears—the corresponding item #26 is isolated as Role = T. The allowed exponent set (excluding forbidden exponents) is:

$$S_{\text{allowed}} = \{2, 3, 4, 6, 8, 10, 11, 12, 17, 20, 42, 48, 68, 70, 104, 204, 208, 291, 300, 600\}. \tag{A.1}$$

Table A.10 Hadron masses (#34–#35).

#	Quantity	ICO formula	ICO	Exp.	Dev.	φ-e	Ly	R	Ty	Dep
34	m_p	$(n{+}1/n)\Lambda_{\mathrm{QCD}}$	943 MeV	938 MeV	0.6%	—	—	D	II	↗8
35	m_p/m_e	$6\pi^5 \times C_{pe}$	1836.2	1836.2	0.002%	—	—	D	II	↗11,34

Table A.11 Gravity and the Planck scale (#36–#38).

#	Quantity	ICO formula	ICO	Exp.	Dev.	φ-e	Ly	R	Ty	Dep
36	G	$\hbar c/(F\varphi^{208}m_e^2)$	$\sim 6.5\times10^{-11}$	6.674×10^{-11}	3.2%	208	E	D	III	↗11
37	M_{Pl}	$\sqrt{F}\,\varphi^{104}\,m_e$	$\sim 1.22\times10^{19}$ GeV	1.22×10^{19} GeV	$\sim$1.6%	104	E	D	III	↗36
38	ρ deviation	$V\alpha/(F\pi)$	$\sim$0.0014	$\sim$0.001	$O(10^{-3})$	—	—	X	III	↗1

Table A.12 Cosmological parameters (#39–#43).

#	Quantity	ICO formula	ICO	Exp.	Dev.	φ-e	Ly	R	Ty	Dep
39	$\Lambda\ell_{\mathrm{Pl}}^2$	φ^{-600}	$\sim10^{-122}$	$\sim10^{-122}$	order	600	E	P	III	—
40	$H_0 t_{\mathrm{Pl}}$	φ^{-291}	$\sim10^{-61}$	$\sim10^{-61}$	1.1%	291	E	P	III	—
41	T_{CMB}/T_Z	φ^{-70}	$\sim3\times10^{-11}$	$\sim3\times10^{-11}$	5.7%	70	E	P	III	—
42	D_{cosmic}	$n{-}1/n = 8/3$	2.667	2.7(±)	$\sim$1%	—	—	P	III	—
43	R_{dS}	$\varphi^{300}\ell_{\mathrm{Pl}}\sqrt{3}$	—	—	—	300	E	D	III	↗39,37

(Items without exponents are marked "—" and are not included in S.)

The statement that "the prohibition rule is stated but the appendix is contradictory" is absorbed and made consistent within the framework of T (negative control). The deviation of factor $\sim$3 in #26 is consistent with the prediction of (P1) that the forbidden index is not physically realized.

A.13.4 Independence / leakage audit

This log does not claim "independence." Instead, it explicitly states dependencies and guarantees that the same information is not counted twice.

A.13.5 Deviation band distribution

A.13.6 Correspondence with SM parameters

Of the 26 free parameters in the SM, 15 have ICO correspondences. Eleven do not: 3 CP phases (A_5 has only real-type representations, L6), 5 large mixing angles ($O(1)$ does not fit the φ-power structure), and 3 individual light quark masses (highly scheme-dependent).

Appendix B Computational Complexity Connections and Systematic Rule Exclusion

This appendix provides details on the connection to computational complexity (Sect. B.1), briefly mentioned in Sect. 3.1, and the systematic elimination of alternative rules in the ρ_4 selection rule (Sects. B.2–B.3) of Sect. 6.2.

B.1 A unified picture of the A_5 barrier in computational complexity

The information barrier created by the non-solvability of A_5 (Theorem 3.1) is structurally parallel to barriers discovered independently in computational complexity and automata theory.

Barrington's theorem [17]. A language L belongs to NC^1 if and only if L is recognized by a polynomial-size, width-5 branching program over A_5. The key point is that when the instruction set is restricted to solvable groups (width 4 or less), the computational power does not reach NC^1. The non-solvability of

Table A.13 Dark components and baryon asymmetry (#44–#46).

#	Quantity	ICO formula	ICO	Exp.	Dev.	φ-e	Ly	R	Ty	Dep
44	$\Omega_{\rm DM}/\Omega_b$	$\lvert A_5\rvert/V=5$	5.0	5.3(1)	$\sim$6%	—	—	X	III	—
45	Ω_Λ	$\varphi^2/(\varphi^2{+}1)$	0.724	0.685	5.7%	—	—	X	III	—
46	η_B	$6\varphi^{-48}$	$\sim 6\times10^{-10}$	$\sim 6\times10^{-10}$	order	48	E	X	III	—

Table A.14 Role breakdown. S and I are made explicit and not mixed into the success rate (blocking selection leakage).

Role	Meaning	Count	Items
I	Input	1	27
S	Selection	2	1, 2
P	Prediction	18	3, 4, 6, 7, 8, 12, 13, 15, 16, 17, 20, 28, 29, 31, 39, 40, 41, 42
D	Derived	14	5, 9, 10, 11, 14, 18, 19, 30, 32, 34, 35, 36, 37, 43
X	Exploratory	10	21, 22, 23, 24, 25, 33, 38, 44, 45, 46
T	Tension	1	26

Table A.15 RG type breakdown. The main argument of the text is Type I (#6, #7) + prohibition structure. Type II/III are downgraded to "research programme."

Type	Meaning	Count	Items
I	RG-independent	2	6, 7
II	Fixed-point hyp.	26	1–5, 11–20, 24–26, 28–35
III	Cosmic freeze-out	17	8–10, 21–23, 36–46
—	Input (no type)	1	27

A_5 creates "computational power that cannot be attained by a solvable sequence of operations." This is the computational-complexity version of Theorem 3.1 (solvable opacity).

Krohn–Rhodes decomposition theorem [18]. Any finite semigroup can be decomposed as an iterated wreath product of prime factors—finite simple groups and reset automata. A_5 is the smallest non-solvable prime in this decomposition, and automata containing A_5 factors cannot be simulated using only solvable primes. While Theorem 3.1 describes the invisibility of A_5 through a homomorphic kernel structure, Krohn–Rhodes describes the same barrier through a wreath product decomposition.

Width criticality and derived series. The "width 5" criticality in Barrington's theorem corresponds directly to the stationarity of the derived series.
Integrated perspective. The four barriers arise from three properties of A_5: (1) non-solvability, (2) simplicity, and (3) minimality ($|A_5| = 60$), and are merely different aspects of the special status of A_5 in the classification of finite simple groups.
Scope limitation. The above structural parallelism is a mathematical fact, not a claim that "computational complexity determines physical laws." The quantitative correspondence between the computational barrier and the physical observation limit remains unresolved as G6.

B.2 Systematic elimination of alternative selection rules

In Sect. 6.2, we showed that the ρ_4 selection rule (C1) $\wedge$ (C2) gives a 10/10 perfect match. In this section, we verify the uniqueness of this rule by predefining the search space and systematically eliminating alternative rules.

Admissible operations and search space. The operations used on the representation ring of A_5 are limited to (i) tensor product $\rho_i \otimes \rho_j$ and its irreducible decomposition, (ii) symmetric power $\mathrm{Sym}^2(\rho_i)$ and alternating power $\Lambda^2(\rho_i)$, and (iii) dimension extraction. The depth is limited to "one tensor product" (Layer C) or "one power operation" (Layer B). There are 10 possible tensor products $\rho_i \otimes \rho_j$ ($i, j \geq 2$, $i \leq j$), and the distinct dimension values are six: $\{9, 12, 15, 16, 20, 25\}$, which are completely predetermined.

Table A.16 Deviation band distribution. The systematic increase from Type I (exact) → Type II (0.1–5%) → Type III (1%–order) is consistent with the classification in Sect. 5.

Deviation band	P	D	X	Representative examples
exact	2	0	0	β_0, quark coefficient
$<1\%$	5	3	0	α_s/α (D), m_t, $\sin^2\theta_W$
1–5%	7	2	2	m_μ/m_e, m_τ/m_e, Λ_{QCD}
$>5\%$ / order	4	9	8	$\Lambda\ell_{\mathrm{Pl}}^2$, T_{CMB}

Table B.1 Width criticality in Barrington's theorem. For width ≤ 4, derived series terminate in finitely many steps. At width 5, A_5—the smallest group whose derived series is stationary ($[A_5, A_5] = A_5$)—becomes available, producing a qualitative leap in computational power. *[Verified.]*

Width	Instruction group candidates	Solvability	NC^1 power
2	C_2 (cyclic)	Solvable	Insufficient
3	$S_3 \cong D_3$ (dihedral)	Solvable	Insufficient
4	S_4 (octahedral)	Solvable	Insufficient
5	A_5 (icosahedral)	Non-solvable	Sufficient

Table B.2 Four manifestations of the A_5 barrier across mathematics, computation, and physics.

Context	Barrier manifestation	Role of A_5	Reference
Group theory (Sect. 3)	A_5 falls entirely in $\ker(\pi)$ of any solvable probe	Smallest solvably invisible group	Thm. 3.1, Cor. 3.1
Computational complexity (Barrington)	Solvable instructions cannot reach NC^1	Critical instruction set for width-5 branching programs	[17]
Automata theory (Krohn–Rhodes)	Cannot be simulated with solvable primes alone	Smallest non-solvable prime	[18]
Physics (Sect. 3.1 + G6)	A_5 structure inaccessible to solvable observers	Minimal basis for irreversibility and information barriers	Cor. 3.3, G6

Elimination of six alternative rules.
Structural reasons for failure. The miss-type failures (Alt-1, 4, 5) are constrained by the SO(3)-derived component and cannot capture the role of ρ_4. The false-accept-type failures (Alt-2, 6) cannot eliminate $\rho_4 \otimes \rho_4 = 16$ (the maximum-entropy decomposition that includes all five irreducible representations once). The ρ_4 participation in (C1) is a representation-theoretic reflection of solvable opacity, and the self-product exclusion in (C2) is equivalent to "decomposition not including ρ_1" by the Schur orthogonality relation.

B.3 Probabilistic assessment and structural reinforcement

Conservative estimate via the hypergeometric distribution. If one randomly assigns 10 tensor products to 6 distinct dimension values, the probability of getting exactly 3 in $\{12, 20\}$ and 7 that do not is $p \approx 0.83\%$. However, due to look-elsewhere effects, this figure alone does not provide strong statistical significance.

Structural arguments beyond statistics. The following three structural facts are more important than probabilistic evaluations:

(i) None of the six alternative rules in Sect. B.2 achieves 10/10, and (C1) ∧ (C2) is the only exact-match rule.

Table B.3 Systematic elimination of alternative selection rules. None achieves 10/10. (C1) ∧ (C2) is the only rule in the examined rule class that gives an exact match.

#	Alternative rule	Match with S	Failure mode
Alt-1	"Products involving ρ_3"	7/10	Miss ($\rho_4 \otimes \rho_5 = 20$)
Alt-2	"Even dimensions only"	8/10	False accept ($\rho_4 \otimes \rho_4 = 16$)
Alt-3	"Non-self-products only"	7/10	Mixed (non-ρ_4 products misaccepted)
Alt-4	"Products involving ρ_5"	7/10	Miss ($\rho_3 \otimes \rho_4 = 12$)
Alt-5	"Dimension ≤ 15"	7/10	Miss ($\rho_4 \otimes \rho_5 = 20$)
Alt-6	"Contains ρ_4" only (no (C2))	8/10	False accept ($\rho_4 \otimes \rho_4 = 16$)

(ii) For each of the forbidden indices $\{9, 15, 16, 25\}$, there is an independent algebraic reason reducing to solvable opacity or the Schur orthogonality relation (Sect. 6.5, Table 20).

(iii) The allowed dimensions $\{12, 20\} = \{V, F\}$ correspond to the number of vertices and faces of the regular icosahedron, revealing a dual correspondence between geometric and tensor product structures.

Connection with exterior algebra. The dimensions $\{1, 4, 6, 4, 1\}$ of the exterior algebra $\Lambda^*(\rho_4) = \bigoplus_{k=0}^{4} \Lambda^k(\rho_4)$ correspond directly to the indices of Layers A–B ($\Lambda^1 = \rho_4$, $\Lambda^2 = \rho_3 \oplus \rho_3'$). Layers A–B are generated by the exterior algebra of ρ_4, and Layer C arises as a tensor product of ρ_4 with other representations. In other words, the entire prohibition structure is derived from the algebraic structure of ρ_4. This structure is structurally parallel to the electron shell system of the hydrogen atom (quantum-number packing rules), but the dynamical basis of the A_5 "power shell" remains unsolved (G4).

Appendix C McKay–E_8 Details, Swampland Correspondence, and Independent Occurrence Contexts of A_5

This appendix provides details of the McKay correspondence (Sects. C.1–C.3), briefly mentioned in Sect. 6.4 of the main text, a systematic comparison with the Swampland program (Sect. C.5), a comparison with Lisi's E_8 unified theory (Sect. C.6), and a survey of contexts in which A_5 appears independently in physics and mathematics (Sect. C.7).

C.1 Extension to SU(2) and the binary icosahedral group

Via the 2:1 covering SU(2) → SO(3), each group in the Klein classification has a double cover.

Table C.1 SO(3) finite subgroups and their SU(2) double covers.

SO(3) subgroup	Order	SU(2) double cover	Order	(H2)	(H3)
C_n	n	C_{2n}	$2n$	✗	—
D_n	$2n$	$2D_n$	$4n$	✗	—
A_4	12	$2T$	24	✓	✗ ($\mathbb{Z}_3$)
S_4	24	$2O$	48	✓	✗ ($\mathbb{Z}_2$)
A_5	60	$2I$	120	✓	✓

Proposition C.1 (Uniqueness in the SU(2) version)**.** Translating the postulates (H1)–(H3) to SU(2) selects $2I$ uniquely.

Argument. C_{2n} and $2D_n$ have reducible two-dimensional defining representations, hence are excluded by (H2). $2T^{\mathrm{ab}} \cong \mathbb{Z}_3$ and $2O^{\mathrm{ab}} \cong \mathbb{Z}_2$, so they are excluded by (H3). $2I$ is a perfect group and its two-dimensional representation is irreducible.

Irreducible representations of $2I$. $2I$ has nine conjugacy classes and nine irreducible representations.

Table C.2 Irreducible representations of $2I$. The five integer-spin representations $(\sigma_1, \sigma_3, \sigma_3', \sigma_4', \sigma_5)$ descend to the five irreducible representations of $A_5 = 2I/\{\pm I\}$.

Symbol	Dimension	Spin	Descent to A_5	McKay node
σ_1	1	Integer	ρ_1	α_0
σ_2	2	Half-integer	✗	α_1
σ_2'	2	Half-integer	✗	α_7
σ_3	3	Integer	ρ_3	α_2
σ_3'	3	Integer	ρ_3'	α_8
σ_4	4	Half-integer	✗	α_3
σ_4'	4	Integer	ρ_4	α_6
σ_5	5	Integer	ρ_5	α_4
σ_6	6	Half-integer	✗	α_5

C.2 McKay correspondence and affine E_8

McKay (1980) [14] discovered a one-to-one correspondence between finite subgroups of SU(2) and extended (affine) Dynkin diagrams. The tensor product decomposition of the two-dimensional defining representation σ_2 with each irreducible representation σ_i,

$$\sigma_2 \otimes \sigma_i = \bigoplus_j a_{ij}\, \sigma_j \,, \tag{C.1}$$

generates an adjacency matrix $A = (a_{ij})$ that encodes an affine Dynkin diagram. For $2I$, the result is the maximal exceptional type $\hat{E}_8$, shown in Fig. C1.

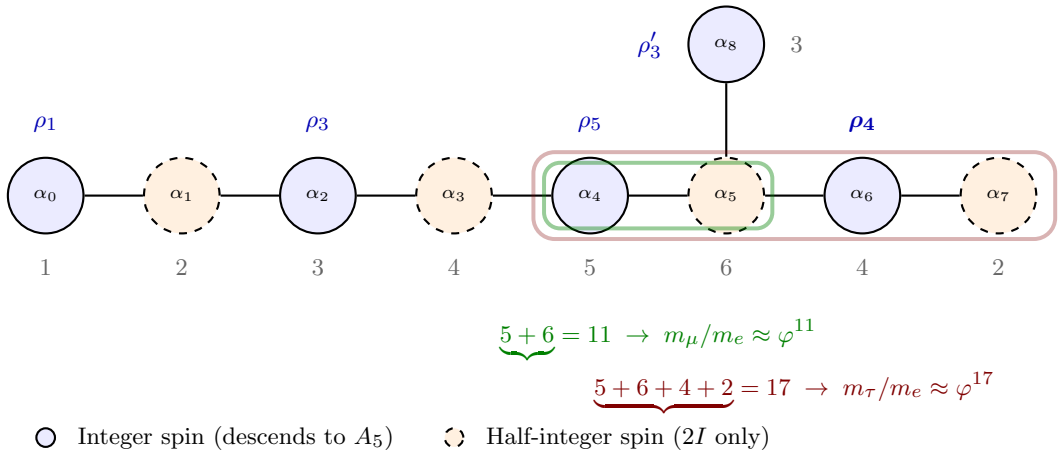

Fig. C1 McKay graph of the binary icosahedral group $2I$, corresponding to the affine Dynkin diagram $\hat{E}_8$. Solid circles (blue) denote integer-spin representations descending to A_5; dashed circles (orange) denote half-integer-spin representations unique to $2I$. Numbers below each node indicate the representation dimension. The branch point α_5 (dim 6) does not descend to A_5. The node α_6 corresponds to ρ_4—the unique non-SO(3) irreducible representation central to the selection rule (P1). Shaded bands indicate the path sums yielding the E_8 Coxeter exponents 11 and 17, which match the charged lepton mass ratios $m_\mu/m_e \approx \varphi^{11}$ and $m_\tau/m_e \approx \varphi^{17}$

The numbers in parentheses are the dimensions of the $2I$-irreducible representations, which correspond to the marks (Dynkin coefficients) of E_8 (Kostant).

Numerical consistency.
A_5-node non-adjacency. On the McKay graph (Fig. C1), the integer-spin nodes $(\alpha_0, \alpha_2, \alpha_4, \alpha_6, \alpha_8)$ descending to A_5 are never adjacent—half-integer-spin nodes $(\alpha_1, \alpha_3, \alpha_5, \alpha_7)$ always act as bridges.

The ρ_4 selection rule in Sect. 6.2—"physical indices require intersection with ρ_4"—can be interpreted as a representation-theoretic reflection of the topological fact that the α_6 node occupies a privileged position on the McKay graph (Fig. C1).

Table C.3 Numerical consistency between E_8 and the icosahedron. The Coxeter number $h(E_8) = 30 = E$ is a necessary consequence of the McKay correspondence.

Quantity	Value
Mark sum $\sum m_i$	$30 = E = h(E_8)$ (Coxeter number)
Mark sum of squares $\sum m_i^2$	$120 = \lvert 2I \rvert$
$\dim(E_8)$	$248 = 8h + 8$
Number of roots	$240 = 4 \times \lvert A_5 \rvert$

Table C.4 McKay graph structure for $\hat{E}_8$. α_6 (corresponding to ρ_4) is topologically special, one step from the branch point α_5. α_5 (dimension $6 = \dim(\Lambda^2\rho_4)$) is unique to $2I$ and does not descend to A_5.

McKay node	Dim.	Spin	A_5 descent	Adjacent nodes
α_0	1	Integer	ρ_1	α_1 (half-int.)
α_1	2	Half-integer	✗	α_0, α_2
α_2	3	Integer	ρ_3	α_1, α_3
α_3	4	Half-integer	✗	α_2, α_4
α_4	5	Integer	ρ_5	α_3, α_5
α_5	6	Half-integer	✗	α_4, α_6, α_8
α_6	4	Integer	ρ_4	α_5, α_7
α_7	2	Half-integer	✗	α_6
α_8	3	Integer	ρ_3'	α_5

C.3 E_8 Coxeter exponents and charged lepton masses

The Coxeter exponents of E_8 are $\mathrm{Exp}(E_8) = \{1, 7, 11, 13, 17, 19, 23, 29\}$. Only $\{11, 17\}$ belong to the allowed set S_{allowed}, and the charged lepton mass ratios $m_\mu/m_e \approx \varphi^{11}$, $m_\tau/m_e \approx \varphi^{17}$ (Appendix A, #12, #13).

Table C.5 Dual membership filter. Only $\{11, 17\}$ are simultaneously E_8 Coxeter exponents and independently derivable icosahedral combinations with established physical correspondences.

E_8 exponent	Icosahedral derivation	Physical quantity	Dual?
1	ρ_1 (trivial repr.)	—	✗
7	$(E+V)/n - 7 = 7$	—	✗ (no indep. A_5 deriv.)
11	$\beta_0 = E/n + \chi/2 = 10 + 1$	$m_\mu/m_e \approx \varphi^{11}$	✓
13	$V + 1$	—	✗ (no indep. phys. match)
17	$F - n = 20 - 3$	$m_\tau/m_e \approx \varphi^{17}$	✓
19	$F - 1$	—	✗ (no indep. phys. match)
23	$F + n$	—	✗ (no indep. phys. match)
29	$E - 1$	—	✗ (no indep. phys. match)

Path structure on the McKay graph. The path sum starting from α_4 ($\sigma_5 \to \rho_5$, dimension 5) produces $\{11, 17\}$ (shaded bands in Fig. C1):

- $11 = m(\alpha_4) + m(\alpha_5) = 5 + 6$: shortest path to the branch point α_5.
- $17 = m(\alpha_4) + m(\alpha_5) + m(\alpha_6) + m(\alpha_7) = 5 + 6 + 4 + 2$: entire path to the arm tip α_7.

Both paths pass through the branch point α_5 (a representation of dimension 6 unique to $2I$ that does not descend to A_5). The charged lepton mass exponents $\{11, 17\}$ are thus simultaneously characterized in three independent contexts: (i) the Coxeter exponents, (ii) physical combinations of the icosahedron, and (iii) path sums on the McKay graph. We leave the elucidation of the dynamical mechanism to G2.

C.4 Path from E_8 to the Standard Model

Physical significance. Proposition C.1 implies that under postulates (H1)–(H3), there is a uniquely determined SU(2) subgroup with a McKay correspondence to E_8. E_8 has a special status in particle physics ($E_8 \times E_8$ in heterotic strings, singularities in F-theory), and this paper provides a new context in which E_8 emerges naturally from holonomy constraints on external spaces.

Candidate route. The typical GUT branching chain is

$$E_8 \supset E_6 \supset \mathrm{SO}(10) \supset \mathrm{SU}(5) \supset \mathrm{SU}(3) \times \mathrm{SU}(2) \times \mathrm{U}(1)\,.$$

The connection path of this paper is

$$A_5 \xrightarrow{\text{Klein}} 2I \xrightarrow{\text{McKay}} E_8 \xrightarrow{\text{GUT}} \mathrm{SM}\,.$$

The first two steps (Klein → McKay) are mathematically rigorous and have been formally verified. The third step (GUT branching) is a physical hypothesis beyond the scope of this paper.

Consistency with superstring theory. While the above GUT branching chain is a field-theoretic pathway, superstring theory provides independent mechanisms for realizing E_8: gauge enhancement at ADE singularities, anomaly cancellation in heterotic strings, and singular fiber degeneracy in F-theory. Our $2I$ (the input of the McKay correspondence) has an entry point consistent with all of these mechanisms. Details are given in Appendix F. This consistency is not an extension of our claims, but a confirmation that the $A_5 \to 2I \to E_8$ chain is consistent with the known framework of string theory.

The essential difficulty. The A_5 holonomy in this paper constrains the exterior space (spatial frame bundle) and does not directly determine the interior gauge symmetry SU(3) × SU(2) × U(1). Three elements are necessary for the connection, and all remain unsolved (G1′).

Table C.6 Three unresolved elements for the external–internal connection (G1′).

Unresolved element	Content	Candidate approaches
External–internal connection	A_5 holonomy → dynamical derivation of gauge group	Kaluza–Klein, spectral geometry
Action functional	Constructing actions consistent with finite group holonomies	Extension of Dijkgraaf–Witten theory [16]
Continuum limit	Discrete holonomy → emergence of continuous fields	Gauge–Higgs unification model

The challenge is not to "derive the gauge group of the SM," but to understand why the algebraic rigidity of A_5 produces SM-like phenomena at low energies.

C.5 Systematic comparison with the Swampland program

The structural consistency with the Swampland conditions, briefly described in Sect. 2.4 of the main text, is systematically listed below.

Classification of satisfaction patterns. The satisfaction of the five Swampland conditions by A_5 holonomy can be classified into three distinct mechanisms.

(i) **Automatic algebraic sufficiency (No-Global-Symmetries, Cobordism).** The single algebraic condition $H^{\mathrm{ab}} = 1$—postulate (H3) itself—automatically satisfies the discrete versions of both conjectures simultaneously.

(ii) **Obvious absence of premise (Distance).** Since discrete holonomy models have no continuous moduli, the assumptions of the Distance Conjecture do not apply.

(iii) **Algebraic description only (Weak Gravity).** The hierarchy $\alpha/\alpha_G \sim \varphi^{204}$ can be described in A_5 algebra, but strict agreement with the quantitative bound of WGC has not been verified.

Global symmetry prohibition in discrete geometry. In continuous gauge theories, the No-Global-Symmetries conclusion is reached via dynamical arguments (such as the black hole no-hair theorem). In discrete holonomies, it is directly enforced by the algebraic structure $H^{\mathrm{ab}} = 1$. When $H^{\mathrm{ab}} \neq 1$, discrete

Table C.7 Systematic comparison of A_5 holonomy with Swampland conjectures.

Swampland conjecture	Content	Relation to A_5	Satisfaction mechanism	What is not claimed
No-Global-Symmetries [11, 12]	No global symmetry in QG	(H3) $H^{\mathrm{ab}} = 1$ prohibits automatic charges	Direct consequence of $H^{\mathrm{ab}} = 1$; A_4 ($\mathbb{Z}_3$) and S_4 ($\mathbb{Z}_2$) eliminated	Proof for continuous gauge theories
Cobordism [13]	Cobordism group is trivial	No nontrivial $H \to \mathrm{U}(1)$ (equivalent to $H^{\mathrm{ab}} = 1$)	Direct consequence of $H^{\mathrm{ab}} = 1$	Complete cobordism computation; strict equivalence
Weak Gravity	Gravity is the weakest force	$\alpha/\alpha_G = \varphi^{204} \sim 10^{44}$	Hierarchy describable in A_5 algebra; quantitative agreement not guaranteed	Rigorous WGC bound derivation
Distance	Infinite tower at large moduli distances	Discrete holonomies have no continuous moduli	Premise of conjecture is absent	Moduli analysis in continuum limit
Finiteness	EFT landscape is finite	Klein's classification limits candidates to five; (H1)–(H3) unify to one	Algebraic finiteness	Counting string vacua

topological charges for closed-curve holonomies are automatically defined independent of dynamics ($\mathbb{Z}_3$ charges in A_4, $\mathbb{Z}_2$ signs in S_4). Postulate (H3) eliminates this algebraically.

C.6 Comparison with Lisi's E_8 unified theory

Lisi (2007) [19] proposed unifying all Standard Model particles into a single Lie algebra by starting directly from the root system of E_8. This approach is fundamentally different from ours in starting point, the status of E_8, methodology, and principal difficulties.

Table C.8 Comparison with Lisi's E_8 theory.

	This paper	Lisi (2007)
E_8 status	$A_5 \to 2I \to$ McKay consequence	Direct assumption
Starting point	3D (H1)(H2)(H3) + frame bundle	E_8 root system + 248-dim. rep.
SM connection	Unresolved (G1′)	Asserted via 248 embedding
Formal verification	Lean 4 (`sorry` = 0)	None
Main difficulty	External–internal gap	Non-embeddability (Distler–Garibaldi)
Scope	Conditional theorem	Theory of Everything

Relationship with the Distler–Garibaldi criticism. The central argument of Distler–Garibaldi [15] against Lisi's proposal was that it is representationally impossible to embed the full particle content of the Standard Model consistently in the root system of E_8. Specifically, the generation structure of fermions and the branching of E_8 representations are incompatible.

Our approach is structurally different from the object of this criticism. We do not directly embed particles in the E_8 root system (we work only with mathematical facts via the McKay correspondence), and we classify the SM connection as unsolved (G1′). All representation-theoretic calculations are formally verified in Lean 4, and our claims are explicitly restricted to conditional theorems.

C.7 Physical and mathematical contexts in which A_5 appears independently

A_5 (the icosahedral group) has a privileged status in multiple physical and mathematical contexts, independent of the three postulates of this paper. The following is an overview, emphasizing that each connection was discovered independently of our framework.

C.7.1 Fibonacci anyons and topological quantum computing

The Fibonacci anyon fusion rule in 2+1-dimensional topological order, $\tau \times \tau = 1 + \tau$, is closely related to the representation theory of A_5. The image of the braid group in SU(2) Chern–Simons theory (level $k = 3$) is homomorphic to A_5 [20], and Fibonacci anyon braiding provides a minimal model for universal quantum computation.

The physical significance is that the non-solvability of A_5 is directly linked to the universality of quantum computation: solvable groups alone limit the simulation capabilities of quantum circuits—this can be seen as the quantum analogue of solvable opacity (Theorem 3.1 in Sect. 3.1) and Barrington's theorem (Appendix B.1).

C.7.2 Barrington's theorem and Krohn–Rhodes theory

As detailed in Appendix B.1, A_5 is the critical instruction set for width-5 branching programs in computational complexity (Barrington [17]) and the smallest "non-solvable prime" of a finite semigroup (Krohn–Rhodes [18]). These results were discovered purely within the theory of computation and algebra, independent of any physical motivation.

C.7.3 Universality of the ADE classification

$2I \to E_8$ corresponds to the most exceptional type in the ADE classification and appears universally in the following contexts.

Table C.9 Universality of the ADE classification and the icosahedral connection.

ADE context	Appearance of E_8	Icosahedral connection
Simple Lie algebras	E_8 is the most exceptional	$2I$ generates $\hat{E}_8$ via McKay
Surface singularity resolution	E_8-type singularity	Orbifold $\mathbb{C}^2/2I$
Heterotic strings	$E_8 \times E_8$ gauge group	10D anomaly cancellation
F-theory	E_8 singular fiber	Compactification geometry
Finite subgroup classification	ADE-compatible maximal example	$2I$ is the largest exceptional subgroup

The universality of the ADE classification shows that the privileged position of E_8 has a mathematical necessity independent of the three postulates of this paper.

C.7.4 Monstrous Moonshine

A_5 is a subgroup of the Monster group $\mathbb{M}$, and McKay's E_8 observation—that E_8 is involved in the factorization of 196883 in the first nontrivial representation of the Monster character table, $196884 = 1 + 196883$—is positioned as part of the $2I \to E_8$ connection and the Moonshine phenomenon. However, a concrete dynamical connection between the framework of this paper and Moonshine has not been established.

C.7.5 Quasicrystals and non-periodic structures

Icosahedral symmetry in three-dimensional space appears directly in materials science as the symmetry of the Penrose tiling (two-dimensional) and quasicrystals (three-dimensional, Shechtman 1984). The five-fold symmetry of quasicrystal diffraction patterns is a geometric realization of A_5, and the golden ratio φ appears in the lattice parameters.

C.7.6 Viral capsid structure

According to the Caspar–Klug theory (1962), most viral capsids (outer shells) exhibit icosahedral symmetry A_5. The T-number (triangulation number) classification is based on the triangulation of icosahedral faces, and the smallest viral capsids ($T = 1$, 60 subunits) directly reflect the A_5 orbit structure.

C.7.7 Implications of independent occurrence

The above contexts were discovered independently of each other and are independent of the three postulates of this paper. The privileged status of $A_5/2I/E_8$ in such a wide variety of contexts suggests that the starting point of this paper (uniqueness via (H1)–(H3)) is not an arbitrary choice but may have reached a mathematically deep structure. However, "appearing in many contexts" does not prove "physically correct," and the epistemological reservation in Sect. 8 applies.

Appendix D Information Barriers, Entropy, and Irreversibility

This appendix details the physical implications of the information barrier briefly mentioned in Sect. 3.1 (solvable opacity).

Epistemological note. The cumulative barrier, minimality, and fiber decomposition in Sect. D.1 are formally verified algebraic facts (Layer M). The physical interpretations in Sects. D.2–D.4 belong to Layer P/E and are speculative. The logical validity of the conditional theorems (Sect. 3) and the prohibition structure (Sect. 6) in the main text is independent of the success or failure of the speculative interpretations in this appendix.

D.1 Quantitative structure of the 60^N information barrier

From Corollary 3.1 and Corollary 3.3, the barriers to solvable observation for A_5 have the following hierarchy:

(I-a) **Existence.** Any solvable probe $\pi\colon A_5 \to Q$ satisfies $\ker(\pi) = A_5$, and 60 microscopic states are mapped to a single observable. *[Verified.]*

(I-b) **Accumulation.** The cumulative ambiguity over N steps grows exponentially to $60^N \geq 2^{5N}$ ($\geq \log_2 60 \approx 5.91$ bits of information loss per step). *[Verified.]*

(I-c) **Minimality.** All finite groups of order less than 60 are solvable and have zero barrier. A_5 defines the minimal basis for irreversibility. *[Verified.]*

(I-a)–(I-c) are pure group-theoretic facts (supported by the classification of finite simple groups [21] and the Feit–Thompson odd-order theorem [22]) and do not depend on physical hypotheses.

Fiber decomposition. By the orbit–stabilizer decomposition in Sect. 4.1.1, 60^N admits three fiber decompositions.

Table D.1 Three fiber decompositions of the 60^N information barrier. The total per step ($\log_2 60 \approx 5.91$ bits) is invariant across sectors; only the orbit/stabilizer partition differs.

Sector	Geom. object	Stabilizer	Orbit bits	Stab. bits	Total
Face (electromagnetic)	$F = 20$	$\mathbb{Z}_3$	≈ 4.32	≈ 1.58	5.91
Edge (strong force)	$E = 30$	$\mathbb{Z}_2$	≈ 4.91	1.00	5.91
Vertex (gravity)	$V = 12$	$\mathbb{Z}_5$	≈ 3.58	≈ 2.32	5.91

There is an anti-correlation between stabilizer-group size (local confinement information) and coupling strength—consistent with the vertex sector (gravitational candidate), which has the largest stabilizer $\mathbb{Z}_5$, being the weakest force. However, the sector correspondence depends on the working hypothesis (C1), and a first-principles derivation has not been achieved (G3).

D.2 Group-theoretic reinterpretation of Boltzmann entropy

In Boltzmann's $S = k_B \ln W$, statistical mechanics explains why W is large by comparing phase-space volumes, but the origin of coarse-graining—why microscopic states become indistinguishable—is usually accepted as a premise. The solvable opacity of A_5 gives an algebraic specification to this origin. Since $\ker(\pi) = A_5$, in N steps:

$$W_N = 60^N\,, \qquad S_N = N\,k_B \ln 60 \approx 4.094\,N\,k_B\,. \tag{D.1}$$

Since A_5 is the smallest non-solvable group (I-c), $\ln 60$ defines the smallest nontrivial lower bound on information loss.

Connection with statistical mechanics. The A_5 framework does not deny statistical mechanics but provides a foundation for it. $W_{\text{total}} \geq W_{\text{dyn}} \times 60^N$, where 60^N is an algebraic factor independent of mechanical details, and W_{dyn} is the conventional phase-space partitioning factor. Ordinary statistical mechanics deals only with W_{dyn}, and 60^N is hidden in the background as the basis for coarse-graining. While Penrose's Past Hypothesis asks "Why did we start from low entropy?", the A_5 framework addresses a logically prior question: "Why is the concept of entropy definable at all?"

D.3 Fourth answer to the Loschmidt paradox

The A_5 framework provides an algebraic answer that is qualitatively different from the three previous answers (Past Hypothesis, typicality, and branching). For microscopic dynamics $g \in A_5$, g^{-1} exists and mechanical reversibility is maintained. However, under any solvable probe $\ker(\pi) = A_5$, so g and g^{-1} become indistinguishable, and the information required to select the "correct inversion operation" vanishes due to the cumulative ambiguity of 60^N in N steps.

If $|H| < 60$, H is solvable, a faithful solvable probe exists, and perfect observational reversibility is maintained. *[Verified.]*

Table D.2 Four answers to the Loschmidt paradox. The A_5 answer addresses the logically prior question of why coarse-graining produces irreversibility.

Answer	Question addressed	Nature
Past Hypothesis	Why low initial S?	Factual
Typicality	Why is S-growth typical?	Measure-theoretic
Branching	Why does the future diverge?	Coarse-graining dependent
A_5 answer	Why does coarse-graining lose information?	Algebraic

D.4 Formal connection with the cosmological constant and the Bekenstein upper bound

For $\Lambda\ell_{\text{Pl}}^2 \sim \varphi^{-600}$ (Appendix A, #39), the exponent 600 has a consistent factorization from information barrier parameters:

$$600 = |A_5| \times 10 = 2 \times 291 + (E - V)\,. \tag{D.2}$$

Internal consistency of the Λ–H_0 relation: $\varphi^{-600} = (\varphi^{-291})^2 \times \varphi^{-18} = \varphi^{-582-18} = \varphi^{-600}$. ✓

Postulates (H1) (finite holonomy) and (H3*) (solvable opacity) independently guarantee two essential properties of entropy:

Table D.3 Dual guarantee of entropy properties from (H1) and (H3*).

Physical principle	Group-theoretic correspondence	Entropy consequence
(H1) Finite holonomy	$N < \infty$	$S \leq N\, k_B \ln 60 < \infty$ (finiteness)
(H3*) Solvable opacity	$\lvert\ker(\pi)\rvert = 60 > 1$	$dS/dN = k_B \ln 60 > 0$ (monotone increase)

D.5 Testability and experimental perspectives

The crucial difference between the A_5 answer and existing answers is the prediction of an irreversibility threshold: $|H| < 60 \;\Rightarrow$ information barrier $= 0 \;\Rightarrow$ no observational irreversibility.

(i) **Quantum simulator.** Comparing the qualitative difference in entropy production rates between A_5 anyon systems and solvable anyon systems (e.g., $\mathbb{Z}_5$). The Fibonacci anyon model (Appendix C.7.1) is the smallest experimental system. [G6]

(ii) **Discrete gauge theory.** Comparison of phase transition structures between $\mathbb{Z}_5$ gauge theory (solvable) and A_5 gauge theory (non-solvable) on the lattice. [G6]

(iii) **Topological quantum computing.** Barrington's theorem [17] mathematically guarantees a qualitative difference in computational power between solvable gauge groups and those including A_5. Whether this difference is physically realized as a difference in entropy production rates is not yet clear. [G6]

D.6 Epistemological summary

Table D.4 Epistemological classification of Appendix D claims.

Claim	Layer	Verification status
Cumulative barrier $60^N \geq 2^{5N}$	M	Lean 4 formally verified
Minimality ($\|G\| < 60 \Rightarrow G$ solvable)	M	Lean 4 formally verified
Three fiber decompositions	M	Lean 4 formally verified
Boltzmann reinterpretation (60^N = coarse-graining lower bound)	P	Speculative
Loschmidt's 4th answer (non-solvability → irreversibility)	P	Speculative
Cosmological constant connection ($600 = 2 \times 291 + 18$)	E	Numerical consistency only
Bekenstein upper bound consistency	P	Speculative

The conditions for falsifying Layer M—(a) the discovery of a non-solvable group of order < 60, (b) the construction of a faithful solvable probe of A_5—have been virtually ruled out by existing mathematical theorems. The conditions for falsifying Layer P/E—(c) the demonstration of a fundamentally reversible macroscopic process, (d) significant deviation between $\Lambda\ell_{\mathrm{Pl}}^2$ and φ^{-600}—are physically open questions left to future experiments and observations.

Appendix E Five Cosmic Constraints — A Unified View

This appendix presents the formulation (Sect. E.1) of the Five Cosmic Constraints (CC1)–(CC5) outlined in Sect. 8.2 of the main text, their logical hierarchy (Sect. E.2), interrelationships and independence (Sect. E.3), and a unified perspective with epistemological summary (Sect. E.4).

Methodological note. The five constraints are structural patterns that emerge when the individual results of Sects. 3–7 are viewed collectively. Each constraint has a different epistemological status (a mixture of Layers M/P/E), and this difference must not be obscured.

E.1 Formulation of the five constraints

The non-solvability of A_5 leads to five hierarchical "cosmic constraints."

CC1: Information barriers and irreversibility. Under A_5 holonomy, solvable observations introduce a structural ambiguity of $|\ker(\pi)| = 60$ at each step, creating a cumulative information barrier of $60^N \geq 2^{5N}$ over N steps. This barrier is an algebraic necessary condition for irreversibility and vanishes in solvable universes with $|H| < 60$.

Physical scope: A possible group-theoretic basis for the second law of thermodynamics; a fourth answer to the Loschmidt paradox (Appendix D.3).

Refutation condition: Demonstration of a macroscopic process that is reversible in principle. (The algebraic facts (I-a)–(I-c) themselves cannot be falsified.)

CC2: Symmetry segmentation and the origin of conservation laws. The action of $A_5 \cong$ Rot(Icosahedron) on the icosahedron uniquely defines three orbits ($F = 20$, $E = 30$, $V = 12$) and stabilizer groups ($\mathbb{Z}_3$, $\mathbb{Z}_2$, $\mathbb{Z}_5$), providing a discrete pre-structure for the three force sectors

(Sect. 4.1.1). The absence of automatic charges due to $H^{\mathrm{ab}} = 1$ can be read as a discrete version of the No-Global-Symmetries Conjecture (Sect. 2.4).

Refutation conditions: (a) Discovery of microscopic universal discrete conserved quantities → (H3) refutation. (b) Discovery of a fourth fundamental force. (c) Empirical denial of the correspondence rule (C1).

CC3: Prohibition structure (algebraic exclusion principle). The representation theory of A_5 defines a threefold prohibition structure for φ-power exponents: (P1) the ρ_4 tensor-product selection rule (10/10 exact match, Sect. 6.2), (P2) the multiplicity-free condition (7/8 match, Sect. 6.3), and (P3) the E_8 Coxeter-exponent filter (Sect. 6.4). The pre-specification of the forbidden exponents $\{9, 15, 16, 25\}$ provides a falsifiable prediction.

Refutation condition: Discovery of stable φ^p relations corresponding to forbidden exponents. Among the five constraints, CC3 has the sharpest falsifiability.

CC4: Necessity of scale hierarchy. The icosahedral parameters $(F, E, V, n) = (20, 30, 12, 3)$ uniquely determine the exponents of all physical scale hierarchies. $H_G = V(F - n) = 204$ (gravitational–electromagnetic hierarchy) is an inevitable consequence of $|A_5| = 60$, and the question "why this hierarchy?" reduces to "why A_5?" All exponents belong to S_{allowed}, which is closed under integer arithmetic on the icosahedral parameters.

Refutation conditions: (a) Discovery of an algebraic structure that realizes an equivalent hierarchy in $n \neq 3$. (b) Discovery of a new scale hierarchy that cannot be described by S_{allowed}.

CC5: Cosmological consistency. The microscopic and macroscopic φ-exponents are consistently connected by integer relations in the icosahedral parameters. The cosmological relation $\Lambda \sim H_0^2$ is automatically satisfied as an internal consistency condition of the A_5 algebra: $600 = 2 \times 291 + (E - V)$, $204 = V \times (F - n)$, $\beta_0 = E/n + \chi/2 = 11$.

Refutation condition: Precision measurements of Λ and H_0 establish systematic deviations from φ^{-600} and φ^{-291}.

E.2 Logical hierarchy

From the non-solvability of A_5, three algebraic mechanisms diverge and crystallize into the five constraints.

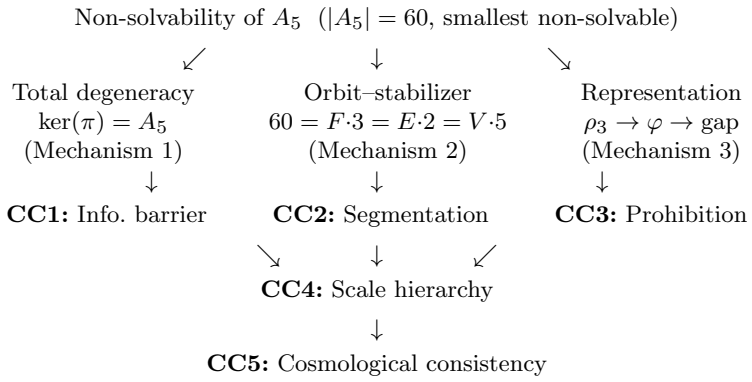

CC1–CC3 arise from the non-solvability of A_5 through three independent algebraic mechanisms. CC4 arises as a quantitative synthesis of CC1–CC3 (barrier "depth" + sector structure + prohibition filter), and CC5 is an extension of CC4 to the macroscale.

E.3 Interrelationships and logical independence

Independence.
Refutation cascade structure.

E.4 Unified perspective and epistemological summary

The five constraints ultimately reduce to a single proposition:

> *A_5 (the alternating group of order 60) is the smallest non-solvable element in the classification of finite simple groups.*

Table E.1 Logical relationships among the five constraints.

Pair	Relation	Basis
CC1 ↔ CC2	Independent	CC1 depends only on non-solvability; CC2 only on orbit decomposition
CC1 ↔ CC3	Independent	Group-theoretic kernel structure vs. representation-theoretic tensor products
CC2 ↔ CC3	Independent	Geometric group action vs. internal structure of the representation ring
CC4 ← CC1–CC3	Subordinate	Combines barrier + prefactor + prohibition structure
CC5 ← CC4	Subordinate	Extension to cosmological scales

Table E.2 Refutation cascade. Rejection of any CC1–CC3 does not affect the others. Rejection of CC4/CC5 has no upstream effect. The five constraints can be verified and refuted individually, not collectively.

Rejected	Downstream effect	Unaffected
CC1	CC4 loses "depth" control	CC2, CC3 unaffected
CC2	CC4 loses sector structure	CC1, CC3 unaffected
CC3	CC4 loses prohibition filter	CC1, CC2 unaffected
CC4	CC5 loses its premise	CC1–CC3 unaffected
CC5	None (terminal node)	CC1–CC4 unaffected

Although these consequences were formulated independently, they derive from a single structure, A_5. This convergence reinforces the motivation for research into G1′ (emergence problem) and G6 (physical realization).

Table E.3 Unified summary of the five cosmic constraints. Although formulated independently, all derive from the single algebraic structure of A_5.

Constraint	Consequence	Physical interpretation	Layer	Falsif.
CC1	Information barrier (60^N)	Possible algebraic basis for the arrow of time	M+P	Medium
CC2	Three-sector force division	Discrete pre-structure of Noether's theorem	M+(C1)	High
CC3	φ-power prohibition structure	Analogue of the Pauli exclusion principle	M	Highest
CC4	Icosahedral arithmetic of scale hierarchies	Possible answer to the hierarchy problem	M+E	Medium
CC5	Micro–macro cosmological alignment	Automatic satisfaction of the Λ–H_0 relation	M+E	Medium

Explicit non-claim. The five constraints do not claim any dynamical mechanism that "determines" the structure of the universe. They are presented as conditional consequences, and each constraint can be evaluated and falsified independently (see Sect. E.3).

Appendix F String Theory Compatibility via E_8

F.1 Purpose and scope

This appendix builds on the mathematical chain established in Sect. 6.4 and Appendix C:

$$A_5 \xrightarrow{\text{Klein}} 2I \xrightarrow{\text{McKay}} \hat{E}_8\,,$$

and checks its structural consistency with the standard constructions of superstring theory. This is not a new physical claim but a compatibility check with known string-theoretic mechanisms.

Note that the McKay correspondence directly gives the affine type $\hat{E}_8$, whereas in string theory "gauge algebra E_8" usually refers to the finite Lie algebra E_8 (the finite part with the affine node removed). This appendix carefully distinguishes the two.

Explicit non-claims. This appendix only presents the structural fact that the mathematical chain $A_5 \to 2I \to E_8$ shares an isomorphic entry point with independent mechanisms on the string theory side. It does not claim the correctness of superstring theory, a string-theoretic derivation of the A_5 holonomy, or a derivation of the SM gauge group.

Layer classification. This appendix belongs to the boundary between Layer M and Layer P. The mathematics of "obtaining E_8 from $2I$"—the McKay correspondence, the algebraic geometry of Du Val/ADE singularities, and the Dechant construction—belongs to Layer M. The interpretation that "it is realized as an effective gauge symmetry of string theory" belongs to Layer P and does not solve the emergence problem G1′ in the main text.

F.2 Three compatibility paths

Our $2I$ (the binary icosahedral group) has an entry point consistent with the following three standard mechanisms in superstring theory.

F.2.1 Path I: ADE singularity and gauge enhancement

In string theory, if the internal space contains an ALE singularity $\mathbb{C}^2/\Gamma$ ($\Gamma \subset \mathrm{SU}(2)$), a gauge algebra corresponding to the ADE classification of Γ is realized on the worldvolume [23].

$\Gamma = 2I$ corresponds to the most exceptional type E_8 in the ADE classification. Therefore:

$$\mathbb{C}^2/2I \longleftrightarrow E_8\text{-type Du Val singularity} \longleftrightarrow E_8 \text{ gauge algebra.}$$

The feature of this path is that E_8 is not a hypothesis but a consequence of $2I$—the double cover of A_5 uniquely determined by (H1)–(H3). Although it does not directly solve L2 (the absence of an external–internal connection), it presents a candidate route in which the exterior holonomy A_5 is reinterpreted as a singularity structure of the internal geometry.

The Du Val singularity $\mathbb{C}^2/2I$ is a simple singularity of type E_8, with canonical form

$$x^2 + y^3 + z^5 = 0\,. \tag{F.1}$$

The exponents $\{2, 3, 5\}$ appearing here correspond to the binary icosahedral group $2I$ as Brieskorn–Pham type data, and simultaneously coincide with the stabilizer orders $\{|\mathrm{Stab}_E|, |\mathrm{Stab}_F|, |\mathrm{Stab}_V|\} = \{2, 3, 5\}$ of the icosahedron (Sect. 4.1.1). Furthermore, in Klein's classical theory [3], the invariant ring of $2I$ has three generators (of degrees 12, 20, 30) with a relation that can be expressed as $f^5 + g^3 + h^2 = 0$ up to rescaling. That $\{2, 3, 5\}$ appears is thus natural from the standpoint of invariant theory (however, this paper does not make a strong claim identifying the variables x, y, z with edges, faces, and vertices).

Layer classification: M (algebraic geometry of Du Val singularities) + P (physical realization of string-theoretic gauge enhancement).

F.2.2 Path II: Heterotic $E_8 \times E_8$ string theory

In heterotic string theory, quantum anomaly cancellation (the Green–Schwarz mechanism [24]) requires that the gauge group be uniquely constrained to $E_8 \times E_8$ or $\mathrm{Spin}(32)/\mathbb{Z}_2$ [25].

Table F.1 Comparison of E_8 emergence: this paper vs. heterotic strings.

	This paper	Heterotic strings
Basis for E_8	(H1)–(H3) $\to A_5 \to 2I \to$ McKay	Anomaly cancellation (10D consistency)
Uniqueness guarantee	Klein classification + 3 principles	Green–Schwarz mechanism
Role of E_8	Filter for prohibition structure (P3)	Gauge symmetry group

It is structurally remarkable that the two "uniquenesses" select the same exceptional Lie algebra from different contexts (3-dimensional discrete geometry and 10-dimensional quantum consistency). However, whether this coincidence is mathematically necessary or accidental is unclear, and we leave its elucidation to G1′ (emergence problem).

In the symmetry breaking of E_8 in heterotic string compactifications, $2I$ can act as follows:

(a) Choose an embedding $2I \hookrightarrow E_8$ and break E_8 to the centralizer $C_{E_8}(2I)$. Whether this centralizer contains a GUT group (such as E_6, SO(10)) is an open question depending on the choice of embedding.

(b) A geometric entry point is to use the Poincaré homology sphere $S^3/2I$ ($\pi_1 \cong 2I$) as a building block of the internal space. This paper does not investigate the consistency conditions in this direction (e.g., anomalies, spectra, moduli).

Layer classification: P (physical hypothesis; specific embedding construction has not been performed).

F.2.3 Path III: E_8-singular fibers of F-theory

In an elliptically fibered compactification of F-theory [26], the type of singular fiber in the Kodaira classification determines the gauge algebra: a type II* singular fiber corresponds to E_8.

Via F-theory/heterotic duality [27, 28], the K3 compactification of F-theory is equivalent to the T^2 compactification of the heterotic string, where an E_8-type singular fiber on K3 corresponds to the E_8 gauge factor on the heterotic side.

The connection to this paper is more indirect than Paths I/II, but in the F-theory framework, E_8 singular fibers arise from the geometric necessity of elliptic curve degeneration—bearing a structural similarity to the "algebraic rigidity of A_5" in this paper.

Layer classification: P (most speculative; based on known dualities in string theory).

F.3 Dechant construction: icosahedral realization of E_8 via Clifford algebra

Independently of the McKay correspondence, Dechant [29] proved that the E_8 root system can be constructed directly from the icosahedral group in the three-dimensional Clifford algebra Cl(3).

Theorem F.1 (Dechant 2016)**.** The set of all pinors (Clifford products of arbitrary numbers of root vectors) of the three-dimensional root system H_3 (the root system of the icosahedral symmetry group) generates 240 eight-component vectors in the eight-dimensional space of Cl(3). Under the contracted inner product, these coincide exactly with the 240 roots of the E_8 root system.

Table F.2 Dimensional ascent in the Dechant construction.

Dimension	Content	String theory correspondence
3	H_3 (icosahedral root system)	Spatial dimension $n = 3$ in this paper
4	H_4 (even subalgebra spinors)	Symmetry group of the regular 120-cell
8	E_8 (full Clifford algebra pinors)	Formal analogy with the transverse 8 of light-cone gauge

The eight-dimensional structure coincides numerically with the kinematic fact of "transverse 8" used in the superstring critical dimension $D = 10 = 2 + 8$ (worldsheet + transverse directions), but this paper does not identify the two; it merely notes a formal similarity. Whether this coincidence is accidental or structural is unclear, and Dechant himself considers this connection speculative.

Table F.3 Complementarity of the McKay and Dechant constructions. Both reach E_8 from the icosahedron via independent paths.

	McKay correspondence	Dechant construction
Input	$2I \subset \mathrm{SU}(2)$	$H_3 \subset O(3)$
Output	Affine $\hat{E}_8$ Dynkin diagram	E_8 root system (240 roots)
Mechanism	Tensor-product adjacency matrix	Pinors of the Clifford algebra
Dim. ascent	$2 \to \mathrm{rank}(E_8) = 8$	$3 \to 8$

The fact that both constructions reach E_8 from the icosahedron via independent paths suggests that this connection is a methodology-independent structural fact.

Layer classification: M (Dechant's theorem itself) + P (correspondence to the transverse dimension in string theory).

F.4 Unified perspective and open problems

The four connection paths are summarized below:

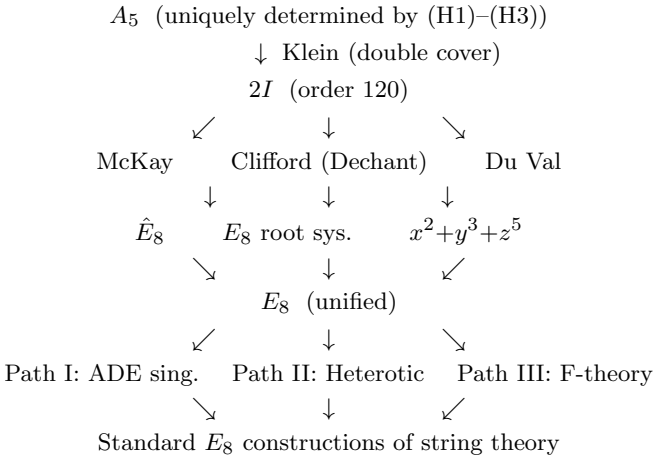

All paths share a common branching point at $2I$ (via McKay or Clifford) and connect to different configurations on the string theory side (ADE singularities, anomaly cancellation, elliptic fiber degeneracy).

Table F.4 Epistemological classification of the four E_8 connection paths.

Path	String theory mechanism	Layer	Specificity
I	ADE singularity → gauge enhancement	M+P	Highest
II	Heterotic $E_8 \times E_8$	P	Medium
III	F-theory II^* fiber	P	Low
—	Clifford construction (Dechant)	M	Complete

F.5 Open problem G7: Specific verification of string theory consistency

As a subproblem of G1′ (emergence problem), we formulate the following as G7.

(G7a) Concrete embedding construction. Construct a concrete embedding $2I \hookrightarrow E_8$ and calculate the centralizer group $C_{E_8}(2I)$. Is the $2I$ embedding naturally realized at any stage of the GUT branching chain $E_8 \supset E_6 \supset \mathrm{SO}(10) \supset \mathrm{SU}(5) \supset \mathrm{SM}$?

(G7b) Compactification interpretation of the prohibition structure. Is the forbidden exponent set $\{9, 15, 16, 25\}$ (Sect. 6.5) naturally excluded in the twisted-sector spectrum of the $2I$ orbifold?

A candidate approach is the analysis of the partition function in the A_5 version of Dijkgraaf–Witten theory [16].

(G7c) Cliffordian origin of the transverse dimension. Can Dechant's $3 \to 8$ dimensional ascent be connected to the dynamical constraints on the critical dimension $D = 10$ of superstring theory (such as central charge $c = 0$)?

Research strategy. G7a is in principle feasible through group-theoretic calculations (e.g., directly computing $C_{E_8}(2I)$ using GAP). G7b lies at the intersection of G4 (index problem) and G1′. G7c is the most speculative and should be preceded by mathematical exploration.

F.6 Epistemological summary

Verification and falsification conditions.

(i) **Path I:** the focus is on whether the external data $(A_5/2I)$ can be implemented as a singularity of the internal geometry and translated into a meaningful low-energy selection rule. If implementation impossibility becomes clear, it will not contribute to the solution of G1′.

(ii) **Path II:** determine whether the centralizer group for the full conjugacy class of $2I \hookrightarrow E_8$ falls near the SM group. If this is not possible by any embedding, Path II is insufficient.

(iii) Dechant's $3 \to 8$ ascent is maintained as a mathematical fact, but if a connection with worldsheet consistency cannot be made, it is treated as a formal similarity.

None of these negative outcomes affects Layer M in the main text.

Explicit non-claims. This appendix is only a consistency check and does not claim to derive A_5 from string theory, nor does it claim that A_5 requires string theory. The usefulness of the string-theoretic continuation depends on progress in G7a–G7c.

References

[1] Moura, L., Ullrich, S.: The Lean 4 theorem prover and programming language. In: Platzer, A., Sutcliffe, G. (eds.) Automated Deduction — CADE 28. Lecture Notes in Computer Science, vol. 12699, pp. 625–635. Springer, Cham (2021). https://doi.org/10.1007/978-3-030-79876-5_37

[2] The mathlib Community: The Lean mathematical library. In: Proceedings of the 9th ACM SIGPLAN International Conference on Certified Programs and Proofs (CPP 2020), pp. 367–381. ACM, New York (2020). https://doi.org/10.1145/3372885.3373824 . Lean 4 API documentation available at https://leanprover-community.github.io/mathlib4_docs/. Accessed 20 Feb 2026

[3] Klein, F.: Vorlesungen über Das Ikosaeder und die Auflösung der Gleichungen Vom Fünften Grade. Teubner, Leipzig (1884). Reprinted: Dover, New York (1956)

[4] Burnside, W.: Theory of Groups of Finite Order, 2nd edn. Cambridge University Press, Cambridge (1911). Reprinted: Dover, New York (2004)

[5] Bekenstein, J.D.: Black holes and entropy. Phys. Rev. D **7**, 2333–2346 (1973) https://doi.org/10.1103/PhysRevD.7.2333

[6] Regge, T.: General relativity without coordinates. Nuovo Cim. **19**, 558–571 (1961) https://doi.org/10.1007/BF02733251

[7] Ambjørn, J., Jurkiewicz, J., Loll, R.: Reconstructing the universe. Phys. Rev. D **72**, 064014 (2005) https://doi.org/10.1103/PhysRevD.72.064014

[8] Rovelli, C., Smolin, L.: Spin networks and quantum gravity. Phys. Rev. D **52**, 5743–5759 (1995) https://doi.org/10.1103/PhysRevD.52.5743

[9] Baez, J.C.: An introduction to spin foam models of BF theory and quantum gravity. In: Gausterer, H., Grosse, H., Pittner, L. (eds.) Geometry and Quantum Physics. Lecture Notes in Physics, vol. 543, pp. 25–93. Springer, Berlin (2000). https://doi.org/10.1007/3-540-46552-9_2

[10] Creutz, M.: Quarks, Gluons and Lattices. Cambridge University Press, Cambridge (1983)

[11] Banks, T., Dixon, L.J.: Constraints on string vacua with spacetime supersymmetry. Nucl. Phys. B **307**, 93–108 (1988) https://doi.org/10.1016/0550-3213(88)90523-8

[12] Harlow, D., Ooguri, H.: Constraints on symmetries from holography. Phys. Rev. Lett. **122**, 191601 (2019) https://doi.org/10.1103/PhysRevLett.122.191601

[13] McNamara, J., Vafa, C.: Cobordism classes and the swampland. J. High Energy Phys. **2021**, 114 (2021) https://doi.org/10.1007/JHEP01(2021)114 1909.10355

[14] McKay, J.: Graphs, singularities, and finite groups. Proc. Symp. Pure Math. **37**, 183–186 (1980)

[15] Distler, J., Garibaldi, S.: There is no "Theory of Everything" inside E_8. Commun. Math. Phys. **298**, 419–436 (2010) https://doi.org/10.1007/s00220-010-1006-y

[16] Dijkgraaf, R., Witten, E.: Topological gauge theories and group cohomology. Commun. Math. Phys. **129**, 393–429 (1990) https://doi.org/10.1007/BF02096988

[17] Barrington, D.A.M.: Bounded-width polynomial-size branching programs recognize exactly those languages in NC^1. J. Comput. System Sci. **38**, 150–164 (1989) https://doi.org/10.1016/0022-0000(89)90037-8

[18] Krohn, K., Rhodes, J.: Algebraic theory of machines. I: Prime decomposition theorem for finite semigroups and machines. Trans. Amer. Math. Soc. **116**, 450–464 (1965) https://doi.org/10.1090/S0002-9947-1965-0188316-1

[19] Lisi, A.G.: An Exceptionally Simple Theory of Everything. Preprint, arXiv:0711.0770 [hep-th] (2007)

[20] Trebst, S., Troyer, M., Wang, Z., Ludwig, A.W.W.: A short introduction to Fibonacci anyon models. Prog. Theor. Phys. Suppl. **176**, 384–407 (2008) https://doi.org/10.1143/PTPS.176.384

[21] Gorenstein, D., Lyons, R., Solomon, R.: The Classification of the Finite Simple Groups. Mathematical Surveys and Monographs, vol. 40. American Mathematical Society, Providence, RI (1994)

[22] Feit, W., Thompson, J.G.: Solvability of groups of odd order. Pacific J. Math. **13**(3), 775–1029 (1963) https://doi.org/10.2140/pjm.1963.13.775

[23] Douglas, M.R., Moore, G.: D-branes, Quivers, and ALE Instantons. Preprint, arXiv:hep-th/9603167 (1996)

[24] Green, M.B., Schwarz, J.H.: Anomaly cancellations in supersymmetric $D = 10$ gauge theory and superstring theory. Phys. Lett. B **149**, 117–122 (1984) https://doi.org/10.1016/0370-2693(84)91565-X

[25] Gross, D.J., Harvey, J.A., Martinec, E., Rohm, R.: Heterotic string. Phys. Rev. Lett. **54**, 502–505 (1985) https://doi.org/10.1103/PhysRevLett.54.502

[26] Vafa, C.: Evidence for F-theory. Nucl. Phys. B **469**, 403–418 (1996) https://doi.org/10.1016/0550-3213(96)00172-1

[27] Morrison, D.R., Vafa, C.: Compactifications of F-theory on Calabi–Yau threefolds I. Nucl. Phys. B **473**, 74–92 (1996) https://doi.org/10.1016/0550-3213(96)00242-8

[28] Morrison, D.R., Vafa, C.: Compactifications of F-theory on Calabi–Yau threefolds II. Nucl. Phys. B **476**, 437–469 (1996) https://doi.org/10.1016/0550-3213(96)00369-0

[29] Dechant, P.-P.: The birth of E_8 out of the spinors of the icosahedron. Proc. R. Soc. A **472**, 20150504 (2016) https://doi.org/10.1098/rspa.2015.0504